

19. Van Gool D, Carmeliet G, Triau E, et al. Appearance of localized immunoreactivity for the $\alpha 4$ integrin subunit and for fibronectin in brains from Alzheimer's, Lewy body dementia patients and aged controls. *Neurosci Lett* 1994;170:71–73
20. Jenkinson ML, Bliss MR, Brain AT, et al. Rheumatoid arthritis and senile dementia of the Alzheimer's type. *Br J Rheumatol* 1989;28:86–88
21. Rogers J, Kirby LC, Hempelman SR, et al. Clinical trial of indomethacin in Alzheimer's disease. *Neurology* 1993;43:1609–11
22. Rich JB, Rasmusson DX, Folstein MF, et al. Nonsteroidal anti-inflammatory drugs in Alzheimer's disease. *Neurology* 1995;45:51–55
23. McGeer PL, Schulzer M, McGeer EG. Arthritis and anti-inflammatory agents as possible protective factors for Alzheimer's disease: A review of 17 epidemiologic studies. *Neurology* 1996;47:425–32
24. Lim GP, Yang F, Chu T, et al. Ibuprofen suppresses plaque pathology and inflammation in a mouse model for Alzheimer's disease. *J Neurosci* 2000;20:5709–14
25. in t' Veld BA, Ruitenbergh A, Hofman A, et al. Nonsteroidal anti-inflammatory drugs and the risk of Alzheimer's disease. *N Engl J Med* 2001;345:1515–21
26. Fiala M, Liu QN, Sayre J, et al. Cyclooxygenase-2-positive macrophages infiltrate the Alzheimer's disease brain and damage the blood-brain barrier. *Eur J Clin Invest* 2002;32:360–71
27. Hoozemans JJ, Bruckner MK, Rozemuller AJ, et al. Cyclin D1 and cyclin E are co-localized with cyclo-oxygenase 2 (COX-2) in pyramidal neurons in Alzheimer disease temporal cortex. *J Neuropathol Exp Neurol* 2002;61:678–88
28. Eriksen JL, Sagi SA, Smith TE, et al. NSAIDs and enantiomers of flurbiprofen target gamma-secretase and lower A β 42 in vivo. *J Clin Invest* 2003;112:440–49
29. Weggen S, Eriksen JL, Sagi SA, et al. A β 42-lowering nonsteroidal anti-inflammatory drugs preserve intramembrane cleavage of the amyloid precursor protein (APP) and ErbB-4 receptor and signaling through the APP intracellular domain. *J Biol Chem* 2003;278:30748–54
30. Smith WL, DeWitt DL, Garavito RM. Cyclooxygenases: Structural, cellular, and molecular biology. *Annu Rev Biochem* 2000;69:145–82
31. Flower RJ, Harvey EA, Kingston WP. Inflammatory effects of prostaglandin D₂ in rat and human skin. *Br J Pharmacol* 1976;56:229–33
32. Hirai H, Tanaka K, Yoshie O, et al. Prostaglandin D₂ selectively induces chemotaxis in T helper type 2 cells, eosinophils, and basophils via seven-transmembrane receptor CRTH2. *J Exp Med* 2001;193:255–61
33. Herve M, Angeli V, Pinzar E, et al. Pivotal roles of the parasite PGD₂ synthase and of the host D prostanoid receptor 1 in schistosome immune evasion. *Eur J Immunol* 2003;33:2764–72
34. Whittle BJ, Moncada S, Vane JR. Comparison of the effects of prostacyclin (PGI₂), prostaglandin E₁ and D₂ on platelet aggregation in different species. *Prostaglandins* 1978;16:373–88
35. Hirata M, Kakizuka A, Aizawa M, et al. Molecular characterization of a mouse prostaglandin D receptor and functional expression of the cloned gene. *Proc Natl Acad Sci U S A* 1994;91:11192–96
36. Lehmann JM, Lenhard JM, Oliver BB, et al. Peroxisome proliferator-activated receptors α and γ are activated by indomethacin and other non-steroidal anti-inflammatory drugs. *J Biol Chem* 1997;272:3406–10
37. Pasinetti GM, Aisen PS. Cyclooxygenase-2 expression is increased in frontal cortex of Alzheimer's disease brain. *Neuroscience* 1998;87:319–24
38. Ueno N, Murakami M, Tanioka T, et al. Coupling between cyclooxygenase, terminal prostanoid synthase, and phospholipase A₂. *J Biol Chem* 2001;276:34918–27
39. Matsuoka T, Hirata M, Tanaka H, et al. Prostaglandin D₂ as a mediator of allergic asthma. *Science* 2000;287:2013–17
40. Matsushita N, Aritake K, Takada A, et al. Pharmacological studies on the novel antiallergic drug HQL-79: II. Elucidation of mechanisms for antiallergic and antiasthmatic effects. *Jpn J Pharmacol* 1998;78:11–22
41. Aritake K, Kado Y, Inoue T, et al. Structural and functional characterization of HQL-79, an orally active, selective inhibitor for human hemopoietic prostaglandin D synthase. *J Biol Chem* 2006;281:15277–86
42. McCullough L, Wu L, Haughey N, et al. Neuroprotective function of the PGE₂ EP2 receptor in cerebral ischemia. *J Neurosci* 2004;24:257–68
43. Bilak M, Wu L, Wang Q, et al. PGE₂ receptors rescue motor neurons in a model of amyotrophic lateral sclerosis. *Ann Neurol* 2004;56:240–48

Lipocalin-type prostaglandin D synthase/ β -trace is a major amyloid β -chaperone in human cerebrospinal fluid

Takahisa Kanekiyo^{*†}, Tadato Ban[‡], Kosuke Aritake^{*}, Zhi-Li Huang^{*5}, Wei-Min Qu^{*}, Issay Okazaki^{*}, Ikuko Mohri^{*¶}, Shigeo Murayama^{||}, Keiichi Ozono[‡], Masako Taniike[¶], Yuji Goto[‡], and Yoshihiro Urade^{*,**}

^{*}Department of Molecular Behavioral Biology, Osaka Bioscience Institute, Suita, Osaka 565-0874, Japan; [†]Department of Pediatrics and [¶]Mental Health and Environmental Effects Research, The Research Center for Child Mental Development, Graduate School of Medicine, and [‡]Institute for Protein Research, Osaka University and CREST Japan Science and Technology Agency, Suita, Osaka 565-0871, Japan; ⁵State Key Laboratory of Medical Neurobiology, Shanghai Medical College of Fudan University, Shanghai 200032, China; and ^{||}Department of Neuropathology, Tokyo Metropolitan Institute of Gerontology, Itabashi-ku, Tokyo 173-0015, Japan

Communicated by Osamu Hayaishi, Osaka Bioscience Institute, Osaka, Japan, February 21, 2007 (received for review December 25, 2006)

The conformational change in amyloid β ($A\beta$) peptide from its monomeric form to aggregates is crucial in the pathogenesis of Alzheimer's disease (AD). In the healthy brain, some unidentified chaperones appear to prevent the aggregation of $A\beta$. Here we reported that lipocalin-type prostaglandin D synthase (L-PGDS)/ β -trace, the most abundant cerebrospinal fluid (CSF) protein produced in the brain, was localized in amyloid plaques in both AD patients and AD-model Tg2576 mice. Surface plasmon resonance analysis revealed that L-PGDS/ β -trace tightly bound to $A\beta$ monomers and fibrils with high affinity ($K_D = 18$ – 50 nM) and that L-PGDS/ β -trace recognized residues 25–28 in $A\beta$, which is the key region for its conformational change to a β -sheet structure. The results of a thioflavin T fluorescence assay to monitor $A\beta$ aggregation disclosed that L-PGDS/ β -trace inhibited the spontaneous aggregation of $A\beta$ (1–40) and $A\beta$ (1–42) within its physiological range (1–5 μ M) in CSF. L-PGDS/ β -trace also prevented the seed-dependent aggregation of 50 μ M $A\beta$ with K_i of 0.75 μ M. Moreover, the inhibitory activity toward $A\beta$ (1–40) aggregation in human CSF was decreased by 60% when L-PGDS/ β -trace was removed from the CSF by immunoaffinity chromatography. The deposition of $A\beta$ after intraventricular infusion of $A\beta$ (1–42) was 3.5-fold higher in L-PGDS-deficient mice and reduced to 23% in L-PGDS-overexpressing mice as compared with their wild-type levels. These data indicate that L-PGDS/ β -trace is a major endogenous $A\beta$ -chaperone in the brain and suggest that the disturbance of this function may be involved in the onset and progression of AD. Our findings may provide a diagnostic and therapeutic approach for AD.

aggregation | Alzheimer's disease | mouse | surface plasmon resonance | thioflavin T

The conformational change in amyloid β ($A\beta$) peptides, $A\beta$ (1–40) and $A\beta$ (1–42), from their soluble monomeric forms to insoluble aggregates is central to the pathogenesis of Alzheimer's disease (AD). $A\beta$ (1–42) peptide is probably the pathogenic one in AD (1–3). Mutations in either amyloid precursor protein or presenilin 1 and 2 genes result in $A\beta$ overproduction (1–3) and have been detected in early onset familial cases of AD, which account for \approx 3% of AD patients (4, 5). In contrast, $A\beta$ production in late-onset sporadic cases of AD, which represent the majority of AD cases, remains unchanged, yet the aggregation of $A\beta$ is enhanced. Functional abnormalities in the deterrents against $A\beta$ aggregation would seem, therefore, to be involved in the pathogenesis of sporadic AD. $A\beta$ is secreted into human cerebrospinal fluid (CSF) under normal conditions (6), and in the healthy brain, it appears to be efficiently controlled by some unidentified extracellular chaperones so as not to aggregate. In the present study, we focused on the possibility of lipocalin-type prostaglandin D synthase (L-PGDS) (7, 8), a major human CSF protein known as β -trace (9), being such a chaperone that functions to prevent $A\beta$ misfolding and aggregation.

Results

Immunostaining of L-PGDS/ β -Trace in Amyloid Plaques. When we immunostained for L-PGDS/ β -trace in the brain of 2-year-old male AD model Tg2576 mice, L-PGDS/ β -trace was detected in many amyloid plaques (Fig. 1A, arrowheads, and B, asterisk), as well as in the leptomeninges (Fig. 1A, small double arrow) as described previously (10, 11). The L-PGDS/ β -trace immunoreactivity was not observed in amyloid plaques when preabsorbed antibody was used (Fig. 1C). Double immunofluorescence staining with anti- $A\beta$ antibody (Fig. 1D) and anti-L-PGDS/ β -trace antibody (Fig. 1E) also revealed that L-PGDS/ β -trace was localized in $A\beta$ -positive amyloid plaques (Fig. 1F, asterisks). In the brain of a late-onset sporadic AD patient, we also confirmed that L-PGDS/ β -trace was immunohistochemically detectable in senile plaques in the frontal cortex (Fig. 1G, arrowheads, and H, asterisk). These data suggest that L-PGDS/ β -trace may bind to $A\beta$ fibrils.

Binding of L-PGDS/ β -Trace to $A\beta$ Peptides. To investigate the binding of L-PGDS/ β -trace to $A\beta$ peptides, we monitored the changes in molecular mass of $A\beta$ (1–40) immobilized on a sensor chip after infusion of various concentrations of L-PGDS/ β -trace solution on the chip by surface plasmon resonance (SPR) analysis. L-PGDS/ β -trace purified from human CSF rapidly bound to the immobilized $A\beta$ (1–40) in a dose-dependent manner and thereafter very slowly dissociated from it after washing with 50 mM sodium phosphate (pH 7.5) and 100 mM NaCl. According to the association and dissociation kinetics, the dissociation constant (K_D) value for the binding affinity was calculated to be 50 nM (Fig. 2A). Conversely, $A\beta$ (1–40) monomer also bound to the immobilized L-PGDS/ β -trace with a similar high affinity at the K_D value of 60 nM (Fig. 2B). L-PGDS/ β -trace also bound to immobilized $A\beta$ (1–42), $A\beta$ (1–40) fibrils, and $A\beta$ (1–42) fibrils with high affinities ($K_D = 40$ – 43 nM; Table 1).

To address which regions of $A\beta$ were involved in the binding to L-PGDS/ β -trace, we used several segments of $A\beta$ peptides for SPR analysis. L-PGDS/ β -trace tightly bound to $A\beta$ (25–35) and

Author contributions: T.K., Y.G., and Y.U. designed research; T.K., T.B., K.A., Z.-L.H., W.-M.Q., and I.O. performed research; T.K., Z.-L.H., W.-M.Q., I.M., S.M., K.O., M.T., Y.G., and Y.U. analyzed data; and T.K., Z.-L.H., and Y.U. wrote the paper.

The authors declare no conflict of interest.

Abbreviations: $A\beta$, amyloid β ; AD, Alzheimer's disease; AFM, atomic force microscopy; CSF, cerebrospinal fluid; L-PGDS, lipocalin-type prostaglandin D synthase; SPR, surface plasmon resonance; ThT, thioflavin T.

**To whom correspondence should be addressed. E-mail: uradey@obi.or.jp.

This article contains supporting information online at www.pnas.org/cgi/content/full/0701585104/DC1.

© 2007 by The National Academy of Sciences of the USA

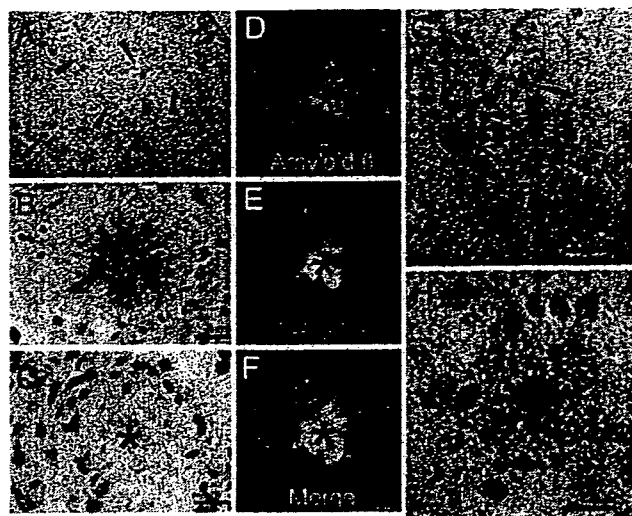


Fig. 1. L-PGDS/β-trace immunostaining of amyloid plaques in Tg2576 mice and AD patients. (A–F) Amyloid plaques in the cerebral cortex of Tg2576 mice (A, arrowheads; B and C, asterisk) were immunopositive with anti-mouse L-PGDS/β-trace antibody (A and B), but not with preabsorbed antibody (C). Double immunofluorescence staining of Aβ (D) and L-PGDS/β-trace (E) showed that they were colocalized (F, merged image). (G and H) In the frontal cortex of a 70-year-old AD patient, amyloid plaques (G, arrowheads; H, asterisk) were immunostained by anti-human L-PGDS/β-trace polyclonal antibody. (Scale bars: A and G, 200 μm; B–F and H, 20 μm.)

Aβ (1–28) peptides with K_D values of 20 and 40 nM, respectively, but not to Aβ (1–16) (Table 1), thus indicating that L-PGDS/β-trace recognized residues 25–28 of Aβ. Recombinant human L-PGDS expressed in *Escherichia coli* also tightly bound to Aβ peptides with K_D values of 18–31 nM.

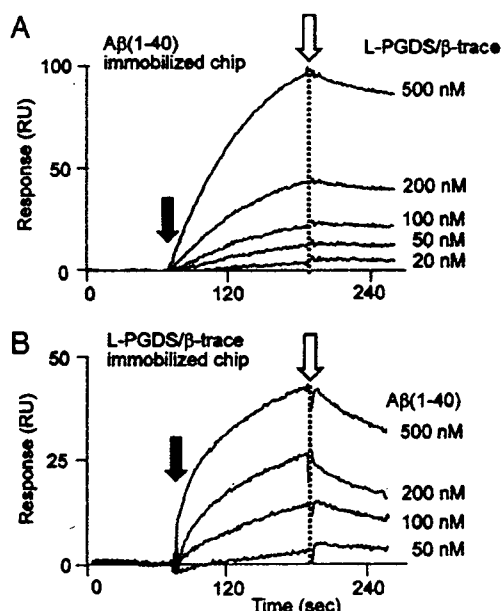


Fig. 2. SPR analysis of binding between L-PGDS/β-trace and Aβ. (A) Binding of L-PGDS/β-trace to 2 ng of immobilized Aβ (1–40). (B) Binding of Aβ (1–40) to 8 ng of immobilized L-PGDS/β-trace. Filled and open arrows show the starting points for sample injection and washing with buffer, respectively. Human serum albumin did not bind to Aβ (1–40) in the same concentration range.

Table 1. K_D values of L-PGDS/β-trace and recombinant L-PGDS to various Aβ peptides by SPR analysis

Peptides	K_D , nM	
	L-PGDS/β-trace	Recombinant human L-PGDS
Aβ (1–40)	50	20
Aβ (1–42)	43	27
Aβ (1–40) fibril	42	31
Aβ (1–42) fibril	40	26
Aβ (25–35)	20	18
Aβ (1–28)	40	19
Aβ (1–16)	Not detected	Not detected

L-PGDS/β-trace purified from human CSF or recombinant human L-PGDS was applied to the various immobilized Aβ peptides. According to the association and dissociation curves, K_D values for the binding affinity were calculated.

Inhibition of Aβ Aggregation by L-PGDS/β-trace *in vitro*. Next, we investigated the effect of L-PGDS/β-trace on spontaneous Aβ aggregation *in vitro* (Fig. 3). The results of a thioflavin T (ThT) fluorescence assay to monitor Aβ aggregation revealed that the fibrillogenesis phase of 50 μM Aβ (1–40) aggregation commenced 24 h subsequent to initiation of the nucleation phase and reached a plateau 48 h thereafter. L-PGDS/β-trace at 1 μM extended the nucleation phase and decreased the final amount of Aβ aggregates to 49% of that in its absence. L-PGDS/β-trace at 5 μM inhibited all spontaneous Aβ aggregation for at least 168 h (Fig. 3A). The fibrillogenesis of Aβ (1–42) commenced even earlier, 6 h after the nucleation phase had begun, and Aβ aggregation reached a plateau within 24 h. L-PGDS/β-trace at 1 μM extended the nucleation phase and decreased the final amount of Aβ aggregates to 62% of that in its absence. The aggregation of Aβ (1–42) was also completely inhibited for at least 168 h in the presence of 5 μM L-PGDS/β-trace (Fig. 3B). The aggregation of both Aβ (1–40) and Aβ (1–42) was prevented in a dose-dependent manner by the addition of either 1 or 5 μM L-PGDS/β-trace, and concentrations are in the physiological range in human CSF (12).

When Aβ fibrils were added as a “seed,” the fibrillogenesis was remarkably accelerated. This seed-dependent aggregation of Aβ was also inhibited by L-PGDS/β-trace [Fig. 3C and D and supporting information (SI) Fig. 7A]. Albumin is the most abundant human CSF protein with the physiological range ≈2–8 μM in human CSF (13). Albumin partially inhibited Aβ aggregation, yet did not completely prevent the seed-dependent aggregation of 50 μM Aβ (1–40) within its physiological range (SI Fig. 7B). Total internal reflection fluorescence microscopy revealed that large Aβ fibrils were produced after incubation of 50 μM Aβ (1–40) monomer with the seed (Fig. 3C Left); however, such fibrils were not observed in the presence of 5 μM L-PGDS/β-trace (Fig. 3C Right). The inhibitory effect of L-PGDS/β-trace on Aβ fibrillogenesis was confirmed by inspection by atomic force microscopy (AFM) (Fig. 3D).

As revealed by circular dichroism (CD) spectrum analysis, the Aβ monomer possessed a predominantly unfolded conformation (Fig. 3E, black). When the Aβ monomer was incubated with a seed, a CD spectrum with a minimum at ≈220 nm appeared, indicating the formation of amyloid fibrils with the β-sheet structure (14) (Fig. 3E, blue). However, in the presence of L-PGDS/β-trace, Aβ did not assume the β-sheet-rich structure (Fig. 3E, red), indicating that L-PGDS/β-trace prevented the conformational change to the β-sheet structure. These results are consistent with the results of the ThT fluorescence assay described above.

The rate of fibrillogenesis of the seed-dependent Aβ (1–40) aggregation was decreased in a concentration-dependent man-

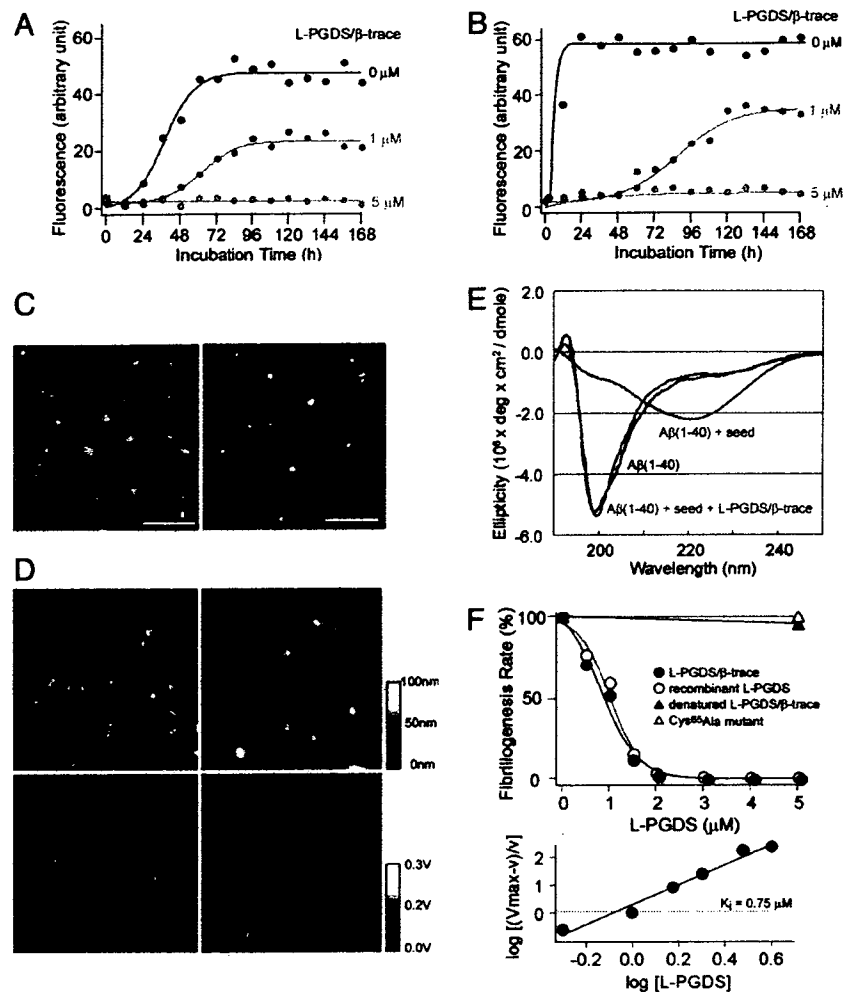


Fig. 3. Inhibition of $A\beta$ aggregation by L-PGDS/ β -trace. (A and B) Spontaneous aggregation of 50 μ M $A\beta$ (1–40) (A) and $A\beta$ (1–42) (B) in the absence (black) or presence of L-PGDS/ β -trace (orange, 1 μ M; green, 5 μ M). (C and D) Observations of $A\beta$ (1–40) seed-dependent aggregation by fluorescence absence (black) or microscopy (C) and AFM (D) in the absence (Left) or presence (Right) of L-PGDS/ β -trace. (Scale bars: C, 10 μ m; D, 1 μ m.) (E) CD spectra of 50 μ M $A\beta$ (1–40) before (black) and after incubation for 2 h with $A\beta$ seed (10 μ g/ml) in the absence (blue) or presence of 5 μ M L-PGDS/ β -trace (red). (F Upper) Inhibition of seed-dependent fibrillogenesis of 50 μ M $A\beta$ (1–40) by incubation for 1 h with L-PGDS/ β -trace purified from human CSF (closed circles), recombinant human L-PGDS (open circles), heat-denatured L-PGDS/ β -trace (closed triangles), or recombinant inactive Cys⁶⁵Ala mutant of human L-PGDS (open triangles). (F Lower) Hill plot of the data obtained for L-PGDS/ β -trace purified from human CSF.

ner by either L-PGDS/ β -trace purified from human CSF or the recombinant L-PGDS (Fig. 3F Upper). The kinetic inhibitory constant (K_i) of L-PGDS/ β -trace with respect to $A\beta$ (1–40) aggregation was calculated by Hill plot analysis to be 0.75 μ M (Fig. 3F Lower). The inhibitory activity against the $A\beta$ (1–40) aggregation was observed with neither heat-denatured L-PGDS/ β -trace nor a recombinant inactive Cys⁶⁵Ala mutant of human L-PGDS (the catalytically active Cys⁶⁵ residue was replaced; Fig. 3F Upper). These results indicate that L-PGDS/ β -trace has a specific conformation required for its interaction with $A\beta$, and that the Cys⁶⁵ residue is crucial for the chaperone activity of L-PGDS/ β -trace to prevent $A\beta$ aggregation.

Preventive Effect of L-PGDS/ β -Trace in Human CSF on $A\beta$ Aggregation.

L-PGDS/ β -trace could be almost completely removed from human CSF by passage through a mouse monoclonal anti-L-PGDS/ β -trace antibody-conjugated column (Fig. 4A). When we compared the inhibitory effect of human CSF and L-PGDS/ β -trace-free CSF on $A\beta$ aggregation, 50% human CSF prevented spontaneous aggregation of $A\beta$ (1–40) for 96 h and 50% L-PGDS/ β -trace-free CSF

for 48 h (Fig. 4B). After incubation for 96 h, human CSF and L-PGDS/ β -trace-free CSF prevented 90% and 36%, respectively, of the spontaneous aggregation of $A\beta$ (1–40), indicating that L-PGDS/ β -trace was the major CSF component responsible for the inhibition of $A\beta$ aggregation (Fig. 4C).

Inhibition of $A\beta$ Deposition by L-PGDS/ β -Trace *in Vivo*.

To test whether L-PGDS/ β -trace could prevent $A\beta$ aggregation *in vivo*, we injected biotin-labeled human $A\beta$ (1–42) into the lateral ventricle of the brain of WT, L-PGDS-knockout (L-PGDS^{-/-}; C57BL/6 strain), and human L-PGDS-transgenic (L-PGDS-Tg; FVB strain) mice. As examined by avidin–biotin–peroxidase staining, deposits of biotin-labeled $A\beta$ (1–42) were detected along the lateral ventricle at 3 h postinjection in all sections examined (Fig. 5). As compared with WT mice (Fig. 5A, C, E, and G), $A\beta$ (1–42) deposition was histologically accelerated in L-PGDS^{-/-} mice (Fig. 5B and F) and reduced in L-PGDS-Tg mice (Fig. 5D and H). Moreover, $A\beta$ deposits were positively stained by Congo-red staining (Fig. 5I–L), indicating that the deposits were composed of $A\beta$ fibrils rather than $A\beta$ monomers.

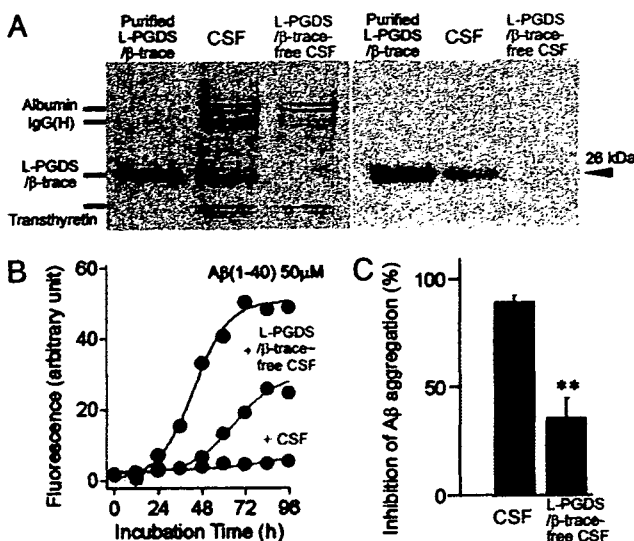


Fig. 4. Inhibitory effect of L-PGDS/β-trace in human CSF on Aβ aggregation. (A) SDS/PAGE and Western blot analysis revealed that L-PGDS/β-trace is a major protein in human CSF with a molecular mass of 26 kDa and is almost completely removed from the CSF by passage through a mouse monoclonal anti-L-PGDS antibody-conjugated column. (B) Representative time course of the spontaneous Aβ aggregation in the absence (black) or presence of 50% human CSF (red) or 50% L-PGDS/β-trace-free CSF (blue). (C) Inhibition of Aβ aggregation in the presence of 50% CSF or the L-PGDS/β-trace-free CSF. The percentage inhibition of Aβ aggregation was calculated by using the formula $[1 - (F_b/F_a)] \times 100$, where F_b and F_a are the ThT fluorescence intensities of 50 μM Aβ (1–40) incubated for 96 h in the presence of 50% CSF or L-PGDS/β-trace-free CSF, respectively. Data are expressed as the mean ± SEM of three independent experiments. **, $P < 0.01$ vs. CSF (Student's *t* test).

Next deposition of Aβ (1–42) was quantified by binding of [¹²⁵I]-streptavidin to brain sections prepared from L-PGDS^{-/-} (7BL/6 strain; Fig. 5M) and L-PGDS-Tg (Fig. 5N) mice and their WT counterparts, and sections had been immunostained with biotin-labeled Aβ (1–42). The deposition of Aβ (1–42) was 3.5-fold higher in L-PGDS^{-/-} mice than in WT mice (Fig. 5M) and 77% lower in L-PGDS-Tg mice than in WT mice (Fig. 5N). These results clearly indicate that L-PGDS/β-trace strongly inhibited Aβ aggregation and deposition *in vivo*.

Discussion

In this study, we demonstrated that L-PGDS/β-trace plays a critical role as an endogenous Aβ-chaperone, thereby inhibiting both Aβ (1–40) and Aβ (1–42) aggregation *in vitro* and *in vivo*. SPR analysis showed that L-PGDS/β-trace tightly bound to Aβ (1–28) and Aβ (25–35), but not to Aβ (1–16), indicating that the hydrophobic region from residues 25–28 of Aβ was crucial for the binding to L-PGDS/β-trace. Interestingly, these same residues in Aβ are the key region for the conformational change in Aβ peptides from the random-coiled to the β-sheet structure (15). During Aβ aggregation, soluble Aβ peptides are known to change their conformation to the β-sheet structure and aggregate to form insoluble fibrils enriched in β-sheet structure (15, 16). The interaction of L-PGDS/β-trace with residues 25–28 in Aβ may prevent this conformational change to the β-sheet structure (Fig. 6), as was suggested by far-UV CD spectrum analysis (Fig. 3E). L-PGDS/β-trace completely prevented Aβ aggregation even at a molar ratio of 1:10. These results suggest that L-PGDS/β-trace catalyzes this conformational change in Aβ from the β-sheet to the random-coiled structure.

The aggregation of Aβ was earlier shown to be inhibited by apolipoprotein (Apo) E (17, 18) and transthyretin (19). Because

of the disturbance of Aβ metabolism (17, 18), ApoE is a risk factor for late-onset AD. The ε4 allele of ApoE shows an incidence of 17.5% among all AD cases (4, 5). However, ApoE is not a CNS-specific protein (13, 20), whereas Aβ is primarily produced in the brain (6, 7). On the other hand, L-PGDS/β-trace is the most abundant CSF protein produced in the brain and is dominantly expressed in the CNS rather than in the peripheral organs. L-PGDS/β-trace exists more abundantly in the brain than ApoE. Furthermore, L-PGDS/β-trace binds to Aβ with an affinity ($K_D = 18$ –50 nM) comparable with that of ApoE ($K_D = 20$ nM) (21). Therefore, L-PGDS/β-trace could be considered more essential than ApoE for the prevention of Aβ aggregation in the brain.

Based on these findings, the incidence of Aβ aggregation would be expected to increase when the L-PGDS/β-trace concentration is decreased or the Aβ-chaperone activity of L-PGDS/β-trace is inactivated in the brain. Two-dimensional gel electrophoresis analysis (22) revealed that L-PGDS/β-trace is decreased in CSF of AD patients as compared with control healthy individuals. In postmenopausal depression, a known risk factor for AD (23), the decrease in the estradiol level is known to elicit a decrease in L-PGDS/β-trace expression (24). In addition, a polymorphism in L-PGDS/β-trace with a C-terminal exon 6-truncation was found in AD patients and claimed to be another risk factor for AD (38). Because C-terminal deletion results in the unfolding and inactivation of L-PGDS/β-trace (25), such mutation is predicted to decrease L-PGDS/β-trace chaperone activity. Moreover, the CSF levels of small hydrophobic molecules such as bilirubin and biliverdin, which bind to L-PGDS/β-trace (26), have been reported to be increased in AD patients (27) and inactivate the Aβ-chaperone activity of L-PGDS/β-trace (T.K., unpublished results). It is reasonable, therefore, to posit that functional disturbances of L-PGDS/β-trace may lead to the sporadic late-onset cases of AD.

Quantitative and qualitative changes in the Aβ-chaperone activity of L-PGDS/β-trace, therefore, may serve as biomarkers for predicting the onset of AD. Further, as the high-resolution x-ray crystallographic structure of L-PGDS has already been determined, it may be possible to design recombinant L-PGDS with a higher affinity for Aβ or to develop novel drugs to increase the affinity of L-PGDS/β-trace for Aβ for use in the therapy of AD. Interestingly, environmental enrichment, as compared with standard animal housing conditions, increased L-PGDS/β-trace gene expression and reduced Aβ deposition in the brain of amyloid precursor protein transgenic mice (28), indicating that the up-regulation of L-PGDS/β-trace may suppress Aβ deposition. That report is in good agreement with our conclusion that L-PGDS/β-trace is the major endogenous Aβ-chaperone to prevent Aβ aggregation in the brain. Our findings thus provide a new insight into the molecular mechanism of AD pathogenesis and a potential therapeutic strategy for AD.

Materials and Methods

Animals. Tg2576 mice (29) were purchased from The Jackson Laboratory (Bar Harbor, ME). L-PGDS^{-/-} mice (30, 31) and human L-PGDS-Tg mice (B20) (32) were generated at the Osaka Bioscience Institute (Osaka, Japan). The experimental protocols employing mice were approved by the Animal Care Committee of Osaka Bioscience Institute, and every effort was made to minimize the number of animals used as well as any pain and discomfort.

Autopsy Brain Tissues. Brain tissues from pathologically diagnosed AD patients were obtained from the Brain Bank of Tokyo Metropolitan Geriatric Hospital and Tokyo Metropolitan Institute of Gerontology (Tokyo, Japan). This study was approved by the institutional review boards of Osaka Bioscience Institute, Tokyo Metropolitan Geriatric Hospital, Tokyo Metropolitan

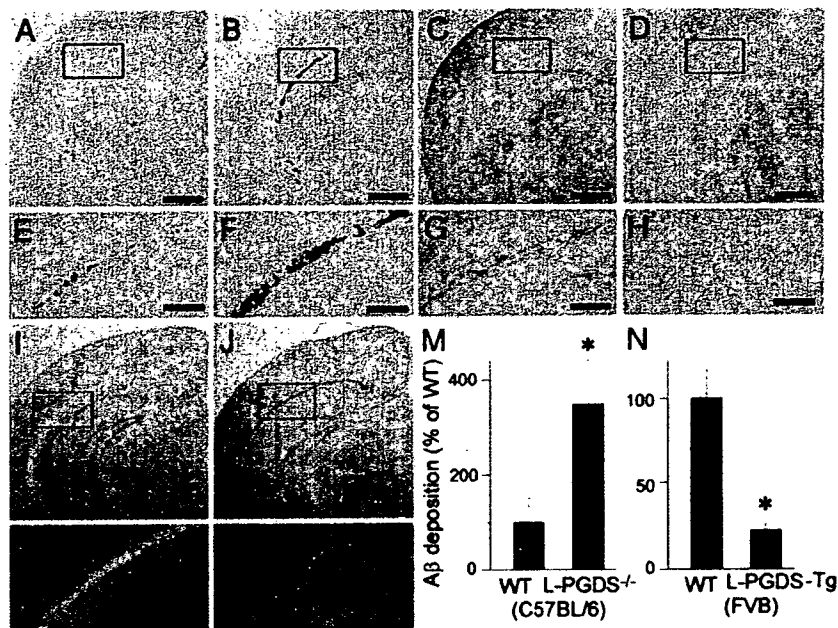


Fig. 5. Inhibition of A β deposition by L-PGDS/ β -trace *in vivo*. (A–H) A β deposition in the brain of WT mice (C57BL/6; A and E), L-PGDS^{-/-} mice (C57BL/6; B and F), WT mice (FVB; C and G), and L-PGDS-Tg mice (FVB; D and H). (Scale bars: A–D, 1 mm; E–H, 200 μ m.) (I–L) Congo-red staining of A β deposition in WT (C57BL/6; I and K) and L-PGDS^{-/-} mice (C57BL/6; J and L) brain as described above. (Scale bar: I and J, 1 mm; K and L, 200 μ m.) (M and N) The A β deposition was quantified by binding of [¹²⁵I]-streptavidin to tissue sections prepared from the brain of WT and L-PGDS^{-/-} mice (C57BL/6; M) and of WT and L-PGDS-Tg mice (FVB; N), which sections had been reacted with biotin-labeled A β (1–42). Data are expressed as the mean \pm SEM ($n = 3$ –4). Significant difference was based on Student's *t* test; *, $P < 0.05$.

Institute of Gerontology, and Osaka University Graduate School of Medicine.

Antibodies. Rabbit polyclonal anti-human L-PGDS (1:1,000 dilution) and anti-mouse L-PGDS (1:4,000 dilution) antisera were raised and purified at the Osaka Bioscience Institute. Monoclonal anti-human A β (11–28) antibody (1:100; IBL, Gunma, Japan) was also used.

Immunohistochemistry. Deparaffinized sections were preincubated with 0.3% H₂O₂ in methanol followed by 50 mM sodium phosphate (pH 7.5) and 100 mM NaCl containing 0.2% Triton X-100. After pretreatment with formic acid for 5 min and trypsin for 15 min, they were sequentially incubated with primary antibody, biotinylated secondary antibody (Vector Laboratories, Burlingame, CA), and avidin–biotin complex (2 μ g/ml; Vector

Laboratories) by using the ABC elite kit according to the manufacturer's protocol. Immunoreactivity was visualized with diaminobenzidine (DAB; Dotite, Kumamoto, Japan) solution. For double immunostaining, deparaffinized sections were incubated at 4°C overnight with anti-A β and anti-L-PGDS antibody, followed by FITC-conjugated anti-mouse IgG (Vector Laboratories) and Texas Red-conjugated anti-rabbit IgG (ICN Biomedicals, Costa Mesa, CA) for 2 h at room temperature.

Preparation of A β Solutions. A β (1–16), A β (25–35), A β (1–40), A β (1–42) (Peptide Institute, Osaka, Japan), and A β (1–28) (AnaSpec, San Jose, CA) were dissolved in 0.02% ammonia solution at 200 μ M. The A β fibril seed solution was prepared by incubation of 50 μ M A β peptides in 50 mM sodium phosphate (pH 7.5) and 100 mM NaCl for 7 days at 37°C.

Purification of Human L-PGDS/ β -Trace in CSF. Human CSF samples were obtained from the Department of Neurosurgery, Nagoya City University Hospital. Informed consent was obtained from all patients for use of their CSF, sampled by lumbar puncture as part of a diagnostic workup. Human L-PGDS/ β -trace was purified from the CSF by immunoaffinity chromatography with a monoclonal anti-human L-PGDS/ β -trace antibody 6F5-conjugated column as reported previously (33).

SPR Analysis. The SPR experiments were performed with a BIAcore 2000 (BIAcore AB, Uppsala, Sweden). A β monomers, fibrils or L-PGDS/ β -trace were immobilized by amine coupling onto a CM5 chip (BIAcore AB) that had been preactivated with a mixture of *N*-ethyl-*N'*-(3-dimethylaminopropyl)carbodiimide hydrochloride and *N*-hydroxysuccinimide. After blocking of the remaining activated carboxyl groups on the sensor chip with ethanolamine, the analyte was applied at a flow rate of 20 μ l/min in 50 mM sodium phosphate (pH 7.5) and 100 mM NaCl at 25°C. Following measurement, the chip surface was regenerated with

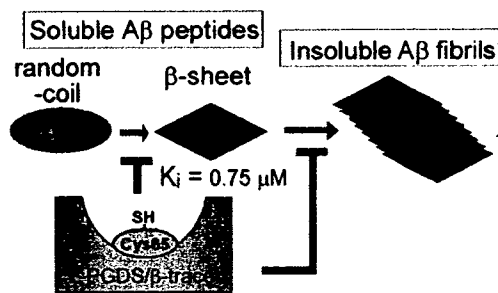


Fig. 6. Proposed schema for inhibition of A β aggregation by L-PGDS/ β -trace. Soluble A β monomers change their conformation from a random-coil dominant structure to the β -sheet-rich structure and then aggregate to insoluble fibrils. L-PGDS/ β -trace can prevent A β aggregation by inhibiting the transformation of A β monomers to β -sheet-rich structure and the sequential seed-dependent A β fibrillogenesis.

50 mM NaOH. The reference cell was prepared by amine coupling without the ligand.

Fluorescence Spectroscopy. A β peptides (50 μ M) were incubated at 37°C in the absence or presence of human L-PGDS/ β -trace purified from human CSF (34), recombinant human L-PGDS expressed in *E. coli* (35), or human CSF in 50 mM sodium phosphate (pH 7.5) and 100 mM NaCl. The seed-dependent and spontaneous A β aggregations were monitored with or without addition of A β seed (final concentration 10 μ g/ml) in a Hitachi F-4500 fluorescence spectrophotometer (Hitachi Software Engineering, Yokohama, Japan) at excitation and emission wavelengths of 446 and 490 nm, respectively, after the components had been mixed with a 200-fold volume of 50 mM glycine-NaOH (pH 8.5) containing 5 μ M ThT (Wako Pure Chemicals, Osaka, Japan) as described earlier (36).

Fluorescence Microscopy and AFM. A β (1–40; 50 μ M) was incubated for 2 h with the A β seed (10 μ g/ml) in 50 mM sodium phosphate (pH 7.5) and 100 mM NaCl in the absence or presence of 5 μ M L-PGDS/ β -trace. The solution was then diluted 5-fold and incubated with ThT of a final concentration of 5 μ M. The fibril formation of A β on glass slides was examined by fluorescence microscopy (37). In the case of AFM, 10 μ l of A β solution was spotted on freshly cleaved mica surfaces and left undisturbed for 2 min, after which the excess solution was blown off with compressed air. AFM images were obtained by using a dynamic force microscope (Nanoscope-RIIIa; Digital Instruments, Santa Barbara, CA).

CD Spectroscopy. A β (1–40) monomer (50 μ M) was dissolved in 50 mM sodium phosphate (pH 7.5) and 100 mM NaCl and incubated in the absence or presence of 5 μ M L-PGDS/ β -trace at 37°C for 2 h. These samples were diluted 2-fold in the buffer

described above, and far-UV CD spectra were recorded at 37°C by using a Jasco-600 spectropolarimeter equipped with a thermostat-controlled cell holder (Jasco, Tokyo, Japan). A quartz cuvette with a 0.1-cm path length was used. The data were presented as the mean residue mass ellipticity for the A β peptide.

Analysis of A β Deposition in Vivo. Under pentobarbital (50 mg/kg, i.p.) anesthesia, biotin-labeled A β (1–42) (100 μ M; AnaSpec, San Jose, CA) was infused at a rate of 0.66 μ l/min for 60 min into the lateral ventricle (coordinates relative to bregma: anterior–posterior 0.0-mm, lateral 2.0-mm, and 2.3-mm depth) of 4-month-old male L-PGDS^{-/-} mice (30, 31) and human L-PGDS-Tg mice (32). At 3 h after administration, the mice were killed. Cryosections (30 μ m) of mouse brain were prepared, fixed in ethanol, and incubated with avidin–biotin–peroxidase complex (2 μ g/ml; Vector Laboratories) according to the manufacturer's protocol. Cryosections were also stained with 1% Congo-red solution. For quantification of A β deposition, cryosections of mouse brain (30 μ m) were fixed in ethanol and incubated with [¹²⁵I]-streptavidin (9.25 kBq/ml, 1,850 kBq/ μ g; Amersham Biosciences, Little Chalfont, U.K.) in 50 mM sodium phosphate (pH 7.5) and 100 mM NaCl for 2 h. After wash by 50 mM sodium phosphate (pH 7.5) and 100 mM NaCl containing 0.2% Triton X-100, the amount of biotin-labeled A β (1–42) within the brain was quantified with a Micro Imager radioisotope detector (Biospace Measures, Paris, France).

SI. Additional results about the inhibition of seed-dependent A β aggregation by L-PGDS/ β -trace or human serum albumin can be found in SI Fig. 7.

We thank Dr. O. Hayaishi for his critical advice in this study, Dr. K. Yamaguchi for help with AFM measurements, and Dr. M. Mase for providing the human CSF samples.

- Sisodia SS (1999) *J Clin Invest* 104:1169–1170.
- Selkoe DJ (2001) *Physiol Rev* 81:741–766.
- Hardy J, Selkoe DJ (2002) *Science* 297:353–356.
- Tanzi RE, Kovacs DM, Kim TW, Moir RD, Guenette SY, Wasco W (1996) *Neurobiol Dis* 3:159–168.
- Tanzi RE (1999) *J Clin Invest* 104:1175–1179.
- Seubert P, Vigo-Pelfrey C, Esch F, Lee M, Dovey H, Davis D, Sinha S, Schlossmacher M, Whaley J, Swindlehurst C, et al. (1992) *Nature* 359:325–327.
- Urade Y, Hayaishi O (2000) *Biochim Biophys Acta* 1482:259–271.
- Urade Y, Eguchi N, Hayaishi O (2006) in *Lipocalins*, ed Akerstrom B, Borregaard N, Flower D, Salier JP (Eurekah.com, Georgetown, TX), pp 99–109.
- Clausen J (1961) *Proc Soc Exp Biol Med* 107:170–172.
- Urade Y, Kitahama K, Ohishi H, Kaneko T, Mizuno N, Hayaishi O (1993) *Proc Natl Acad Sci USA* 90:9070–9074.
- Beuckmann CT, Lazarus M, Gerashchenko D, Mizoguchi A, Nomura S, Mohri I, Uesugi A, Kaneko T, Mizuno N, Hayaishi O, Urade Y (2000) *J Comp Neurol* 428:62–78.
- Hiraoka A, Arato T, Tominaga I, Anjyo A (1997) *J Pharm Biomed Anal* 15:1257–1263.
- Einstein ER (1982) *Proteins of the Brain and CSF in Health and Disease* (Thomas, Springfield, IL).
- Raman B, Ban T, Sakai M, Pasta SY, Ramakrishna T, Naiki H, Goto Y, Rao Ch M (2005) *Biochem J* 392:573–581.
- Petkova AT, Ishii Y, Balbach JJ, Antzutkin ON, Leapman RD, Delaglio F, Tycko R (2002) *Proc Natl Acad Sci USA* 99:16742–16747.
- Harper JD, Lansbury PT, Jr (1997) *Annu Rev Biochem* 66:385–407.
- Wisniewski T, Frangione B (1992) *Neurosci Lett* 135:235–238.
- Naslund J, Thyberg J, Tjernberg LO, Wernstedt C, Karlstrom AR, Bogdanovic N, Gandy SE, Lannfelt L, Terenius L, Nordstedt C, et al. (1995) *Neuron* 15:219–228.
- Schwarzman AL, Gregori L, Vitek MP, Lyubski S, Strittmatter WJ, Enghilde JJ, Bhasin R, Silverman J, Weisgraber KH, Coyle PK, et al. (1994) *Proc Natl Acad Sci USA* 91:8368–8372.
- Pitas RE, Boyles JK, Lee SH, Hui D, Weisgraber KH (1987) *J Biol Chem* 262:14352–14360.
- Golabek AA, Soto C, Vogel T, Wisniewski T (1996) *J Biol Chem* 271:10602–10606.
- Puchades M, Hansson SF, Nilsson CL, Andreassen N, Blennow K, Davidsson P (2003) *Brain Res Mol Brain Res* 118:140–146.
- Shumaker SA, Legault C, Rapp SR, Thal L, Wallace RB, Ockene JK, Hendrix SL, Jones BN, III, Assaf AR, Jackson RD, et al. (2003) *J Am Med Assoc* 289:2651–2662.
- Mong JA, Devidze N, Frail DE, O'Connor LT, Samuel M, Choleris E, Ogawa S, Pfaff DW (2003) *Proc Natl Acad Sci USA* 100:318–323.
- Urade Y, Tanaka T, Eguchi N, Kikuchi M, Kimura H, Toh H, Hayaishi O (1995) *J Biol Chem* 270:1422–1428.
- Beuckmann CT, Aoyagi M, Okazaki I, Hiroike T, Toh H, Hayaishi O, Urade Y (1999) *Biochemistry* 38:8006–8013.
- Kimpara T, Takeda A, Yamaguchi T, Arai H, Okita N, Takase S, Sasaki H, Itoyama Y (2000) *Neurobiol Aging* 21:551–554.
- Lazarov O, Robinson J, Tang YP, Hairston IS, Korade-Mirnic Z, Lee VM, Hersh LB, Sapolsky RM, Mirnic K, Sisodia SS (2005) *Cell* 120:701–713.
- Hsiao K, Chapman P, Nilsen S, Eckman C, Harigaya Y, Younkin S, Yang F, Cole G (1996) *Science* 274:99–102.
- Eguchi N, Minami T, Shirafuji N, Kanaoka Y, Tanaka T, Nagata A, Yoshida N, Urade Y, Ito S, Hayaishi O (1999) *Proc Natl Acad Sci USA* 96:726–730.
- Qu WM, Huang ZL, Xu XH, Aritake K, Eguchi N, Nambu F, Narumiya S, Urade Y, Hayaishi O (2006) *Proc Natl Acad Sci USA* 103:17949–17954.
- Pinzar E, Kanaoka Y, Inui T, Eguchi N, Urade Y, Hayaishi O (2000) *Proc Natl Acad Sci USA* 97:4903–4907.
- Oda H, Shiina Y, Seiki K, Sato N, Eguchi N, Urade Y (2002) *Clin Chem* 48:1445–1453.
- Oda H, Eguchi N, Urade Y, Hayaishi O (1996) *Proc Jpn Acad* 72:108–111.
- Inui T, Ohkubo T, Emi M, Irikura D, Hayaishi O, Urade Y (2003) *J Biol Chem* 278:2845–2852.
- Naiki H, Higuchi K, Hosokawa M, Takeda T (1989) *Anal Biochem* 177:244–249.
- Ban T, Goto Y (2006) *Methods Enzymol* 413:91–102.
- Fabien S, Annelies R, Laurent D (2004) Unexamined Patent FR2848573A1.

Neuropathologic diagnostic and nosologic criteria for frontotemporal lobar degeneration: consensus of the Consortium for Frontotemporal Lobar Degeneration

Nigel J. Cairns · Eileen H. Bigio · Ian R. A. Mackenzie · Manuela Neumann · Virginia M. -Y. Lee · Kimmo J. Hatanpaa · Charles L. White III · Julie A. Schneider · Lea Tenenholz Grinberg · Glenda Halliday · Charles Duyckaerts · James S. Lowe · Ida E. Holm · Markus Tolnay · Koichi Okamoto · Hideaki Yokoo · Shigeo Murayama · John Woulfe · David G. Munoz · Dennis W. Dickson · Paul G. Ince · John Q. Trojanowski · David M. A. Mann

Received: 9 May 2007 / Accepted: 9 May 2007 / Published online: 20 June 2007
© Springer-Verlag 2007

Abstract The aim of this study was to improve the neuropathologic recognition and provide criteria for the pathological diagnosis in the neurodegenerative diseases grouped as frontotemporal lobar degeneration (FTLD); revised criteria are proposed. Recent advances in molecular genetics, biochemistry, and neuropathology of FTLD prompted the Midwest Consortium for Frontotemporal Lobar Degeneration

and experts at other centers to review and revise the existing neuropathologic diagnostic criteria for FTLD. The proposed criteria for FTLD are based on existing criteria, which include the tauopathies [FTLD with Pick bodies, corticobasal degeneration, progressive supranuclear palsy, sporadic multiple system tauopathy with dementia, argyrophilic grain disease, neurofibrillary tangle dementia, and

N. J. Cairns
Department of Neurology,
Washington University School of Medicine,
Campus Box 8118, 660 South Euclid Avenue,
St Louis, MO 63110, USA

N. J. Cairns (✉)
Department of Pathology and Immunology,
Washington University School of Medicine,
Campus Box 8118, 660 South Euclid Avenue,
St Louis, MO 63110, USA
e-mail: cairns@wustl.edu

N. J. Cairns
Alzheimer's Disease Research Center,
Washington University School of Medicine,
Campus Box 8118, 660 South Euclid Avenue,
St Louis, MO 63110, USA

E. H. Bigio
Department of Pathology,
Northwestern University Feinberg School of Medicine,
Chicago, IL, USA

E. H. Bigio
Cognitive Neurology and Alzheimer Disease Center,
Northwestern University Feinberg School of Medicine,
Chicago, IL, USA

I. R. A. Mackenzie
Department of Pathology and Laboratory Medicine,
Vancouver General Hospital, Vancouver, BC, Canada

M. Neumann
Center for Neuropathology and Prion Research,
Ludwig-Maximilians University, Munich, Germany

V. M.-Y. Lee · J. Q. Trojanowski
Department of Pathology and Laboratory Medicine,
Center for Neurodegenerative Disease Research,
University of Pennsylvania School of Medicine,
Philadelphia, PA, USA

J. Q. Trojanowski
Institute on Aging,
University of Pennsylvania School of Medicine,
Philadelphia, PA, USA

K. J. Hatanpaa · C. L. White III
Neuropathology Laboratory, Department of Pathology,
University of Texas Southwestern Medical School,
Dallas, TX, USA

J. A. Schneider
Rush Alzheimer's Disease Center,
Rush University Medical School,
Chicago, IL, USA

L. T. Grinberg
Department of Pathology and Instituto Israelita
de Ensino e Pesquisa Albert Einstein, Faculdade
de Medicina, Universidade de São Paulo, Sao Paulo, Brazil

FTD with *microtubule-associated tau (MAPT)* gene mutation, also called FTD with parkinsonism linked to chromosome 17 (FTDP-17)]. The proposed criteria take into account new disease entities and include the novel molecular pathology, TDP-43 proteinopathy, now recognized to be the most frequent histological finding in FTLN. TDP-43 is a major component of the pathologic inclusions of most sporadic and familial cases of FTLN with ubiquitin-positive, tau-negative inclusions (FTLN-U) with or without motor neuron disease (MND). Molecular genetic studies of familial cases of FTLN-U have shown that mutations in the *progranulin (PGRN)* gene are a major genetic cause of FTLN-U. Mutations in *valosin-containing protein (VCP)* gene are present in rare familial forms of FTD, and some families with FTD and/or MND have been linked to chromosome 9p, and both are types of FTLN-U. Thus, familial TDP-43 proteinopathy is associated with defects in multiple genes, and molecular genetics is required in these cases to correctly identify the causative gene defect. In addition to genetic heterogeneity amongst the TDP-43 proteinopathies, there is also neuropathologic heterogeneity and there is a close relationship between genotype and FTLN-U subtype. In addition to these recent significant advances in the neuropathology of FTLN-U, novel FTLN entities have been further characterized, including neuronal intermediate filament inclusion disease. The proposed criteria incorporate up-to-date neuropathology of FTLN in the light of recent immunohistochemical, biochemical, and genetic

advances. These criteria will be of value to the practicing neuropathologist and provide a foundation for clinical, clinico-pathologic, mechanistic studies and in vivo models of pathogenesis of FTLN.

Keywords Frontotemporal dementia · Semantic dementia · Progressive non-fluent aphasia · Frontotemporal lobar degeneration · Motor neuron disease · Tauopathy · Ubiquitin · TDP-43 proteinopathy · Progranulin · Valosin-containing protein · Charged multivesicular body protein 2B · Neuronal intermediate filament inclusion disease · Neuropathologic diagnosis

Introduction

In this paper, we follow the convention that FTLN is an umbrella term that groups several different neurodegenerative diseases characterized by predominant destruction of the frontal and temporal lobes. After Alzheimer disease (AD) and dementia with Lewy bodies (DLB), frontotemporal lobar degeneration (FTLN) is the third most common neurodegenerative cause of dementia in industrialized countries [59, 60, 69]. Most commonly, patients with FTLN present with frontotemporal dementia (FTD), a change in personal and social conduct, often associated with disinhibition, with gradual and progressive changes in language [53]. Other patients falling under the diagnostic umbrella of FTLN may

G. Halliday
Prince of Wales Medical Research Institute,
Sydney, NSW, Australia

C. Duyckaerts
Laboratoire de Neuropathologie Escourrolle,
Hôpital de La Salpêtrière, Paris, France

J. S. Lowe
Department of Neuropathology, Queen's Medical Centre,
Nottingham University Hospitals NHS Trust, Nottingham, UK

I. E. Holm
Department of Pathology, Aalborg Hospital,
Aarhus University Hospital, Aalborg, Denmark

M. Tolnay
Department of Neuropathology, Institute of Pathology,
University Hospital Basel, Basel, Switzerland

K. Okamoto
Department of Neurology,
Gunma University Graduate School of Medicine,
Maebashi, Gunma, Japan

H. Yokoo
Department of Human Pathology,
Gunma University Graduate School of Medicine,
Maebashi, Gunma, Japan

S. Murayama
Geriatric Neuroscience (Neuropathology),
Tokyo Metropolitan Institute of Gerontology,
Itabashi, Tokyo, Japan

J. Woulfe
Department of Pathology,
Ottawa Hospital and University of Ottawa,
Ottawa, ON, Canada

D. G. Munoz
Department of Pathology,
Saint Michael's Hospital and University of Toronto,
Toronto, ON, Canada

D. W. Dickson
Neuropathology Laboratory,
Mayo Clinic College of Medicine,
Jacksonville, FL, USA

P. G. Ince
Neuropathology Group, Academic Unit of Pathology,
University of Sheffield Medical School, Sheffield, UK

D. M. A. Mann
Clinical Neuroscience Research Group,
School of Translational Medicine,
Greater Manchester Neurosciences Centre,
University of Manchester, Salford, UK

present with early and progressive changes in language function, and two syndromes have been recognized: semantic dementia (SD) and primary progressive non-fluent aphasia (PNFA) [40, 43, 53, 65, 67, 78]. In later stages of these particular syndromes, both behavioral and language dysfunction may be present. A proportion of patients with FTLD present with or develop parkinsonism as part of their disease process. Clinical amyotrophic lateral sclerosis/motor neuron disease (ALS/MND) may also be found in a proportion of patients with FTLD, especially those with FTD, indicating a spectrum of clinical phenotypes that relate to common neuropathologic lesions [3, 61, 69].

FTD, SD, or PNFA refer to the main clinical syndromes linked to the FTLD group. Typically, at least in the early course of the disease, patients with FTD do not have an amnesic syndrome, which distinguishes them clinically from AD [46, 53], but there are exceptions [29]. Although no pre-symptomatic biomarkers have been identified, at least in sporadic cases, clinical assessment, neuropsychology, and neuroimaging may help to distinguish FTD and the related disorders of SD and PNFA from other neurodegenerative causes of dementia [12, 43, 46]. The diagnosis of FTD, SD, or PNFA may only be considered when other potential causes of dementia including other nervous system diseases (e.g., small and large vessel disease), systemic conditions (e.g., hypothyroidism), tumors, and substance abuse have been excluded.

The *apolipoprotein E (APOE)* gene $\epsilon 4$ allele is a major risk factor for AD, though this is not the case in most association studies of FTLD (but see ref. [71]), and none of the autosomal dominant mutations in genes associated with some familial cases of AD [*amyloid precursor protein (APP)*, *presenilin 1 (PS1)* and *presenilin 2 (PS2)*] acts as a risk factor for FTLD.

Recent developments in the molecular pathology and genetics of FTLD now dictate that a minimal panel of pathological investigations is required for correct diagnosis in this group of diseases. Standardization of nomenclature and approach will facilitate better understanding of clinico-pathologic correlations, provide insights into pathogenesis, and guide the construction and validation of *in vivo* models.

Neuropathologic evaluation

With the exception of those cases in which a gene defect has been identified, examination of the brain and neuropathology are essential in order to determine the disease entity underlying FTLD. Even in those cases that have been genetically characterized, it is not uncommon to find coexisting neurodegenerative disease and other pathology, which may have contributed to the clinical picture to a varying degree. The neuropathology of the brain, either on autopsy or, rarely, on

biopsy, remains the “gold standard” for determining the neuropathologic diagnosis. Although most cases seen by a neuropathologist are likely to be cases of advanced disease, there is an increasing awareness that the molecular pathology of all neurodegenerative disease is present often several years prior to the onset of clinical symptoms, and this knowledge will inform the neuropathologist of pre-clinical FTLD in an otherwise cognitively and behaviorally normal subject.

Macroscopy

Examination of the brain of a patient with FTLD typically shows symmetrical focal atrophy of the frontal or temporal lobes, or both. In some patients there is asymmetry of atrophy, typically reflected in perisylvian loss on one side of the brain. Macroscopic atrophy of the basal ganglia and loss of pigmentation from the substantia nigra are seen in a proportion of cases. This focal atrophy is, not infrequently, the most dramatic in all of neuropathology. Conversely, in some individuals, for example, those who die at an earlier stage, the brain is unremarkable. The pattern of atrophy may assist in staging disease severity [11, 39, 41].

Microscopy

In most forms of FTLD, examination of the cerebral cortex with H&E staining shows microvacuolation and neuronal loss. In many cases, this is most evident around layer II of the affected cortical regions. In advanced cases, there is transcortical microvacuolation and neuronal loss. Swollen cortical neurons may be seen and highlighted with immunostaining for alpha B-crystallin; however, they are not specific for any disease subtype. White matter myelin loss and astrocytic gliosis may be seen. There may be significant neuronal loss from the basal ganglia and substantia nigra in some cases.

Specific diagnosis of disease within the broad group of FTLD now requires immunohistochemistry (IHC) to determine the molecular pathology, morphology, and distribution of lesions in the neuraxis, and thereby identify the neurodegenerative disease. In the routine microscopic evaluation of the brain of a patient with FTLD, other neurodegenerative diseases may be identified, most commonly AD [18], DLB [52], and, rarely, prion disease [33] and hereditary diffuse leukoencephalopathy with axonal spheroids [76].

Although some neurodegenerative diseases can be readily identified using conventional staining techniques (e.g., modified Bielschowsky and Gallyas silver impregnations and thioflavine-S for AD pathology [8, 18, 54]), more sensitive and reliable IHC techniques are now preferred. IHC methods are more consistent and dependable than are silver impregnation techniques, they have greater inter-rater reliability, as shown by the BrainNet Europe Consortium study [1], and IHC results can suggest or identify underlying molecular pathology.

For example, antibodies raised against epitopes of tau readily label the neurofibrillary tangles, neuritic plaques, and neuropil threads of AD; anti- β -amyloid antibodies detect diffuse and compact β -amyloid deposits and cerebral amyloid angiopathy [10]; while anti- α -synuclein antibodies label Lewy bodies and Lewy neurites, the signature lesions of DLB [10, 52]. Neuropathologic staging schemes have been developed using tau, β -amyloid and α -synuclein IHC, and IHC is now replacing conventional stains in the neuropathologic diagnostic criteria for AD and DLB [10, 18, 52]. Prion IHC may be used reliably to detect or exclude prion disease in most cases [33]. Proteins targeted for degradation are ubiquitinated and several hallmark inclusions in neurodegenerative disease either in neurons or glia or both are detected by ubiquitin IHC [17, 19, 47, 48]. There is also age-related accumulation of ubiquitinated material in the brain [23], which can make detection of certain ubiquitin-related pathologies difficult. Until recently, ubiquitin IHC was the only marker for certain neuronal inclusions seen in FTLD and ALS/MND that contained neither tau nor α -synuclein epitopes. P62 (sequestosome-1) IHC has recently been highlighted as an alternative method to detect a range of ubiquitin-immunoreactive structures in neurodegenerative diseases including ALS/MND, and FTLD. Like ubiquitin IHC, a range of pathological and age-related abnormalities are detected, but an advantage over anti-ubiquitin IHC appears to be that there is better contrast in the detection of intracellular pathology. More recently, TDP-43 has been identified as a major component of the inclusions of FTLD with ubiquitin-positive, tau- and α -synuclein-negative inclusions (FTLD-U) [3, 61], formerly called FTLD with MND-type inclusions, but without MND [53]. This protein now defines a novel class of neurodegenerative diseases collectively called TDP-43 proteinopathies [16], and TDP-43 IHC may be used to characterize a majority of FTLD-U, but not all [16].

Although IHC is essential for determining the underlying molecular pathology of the majority of neurodegenerative diseases, other techniques may be available in dementia research centers and complement the routine neuropathologic diagnosis. The reliable and robust detection of abnormally aggregated proteins either within neurons or glia or both, or in the neuropil, is necessary for neuropathologic diagnosis. However, the density and distribution of abnormal protein aggregates, as identified by IHC, do not always correlate well with clinical symptoms. Other markers, such as synaptic and neuronal loss in affected brain areas, may correlate better with cognitive impairment and motor dysfunction. Thus, stereologic methods that assess synaptic and neuronal loss in an unbiased manner may be useful in clinico-pathologic studies in the dementia research center, but are not necessary, or usually feasible, for routine neuropathologic diagnosis.

Biochemistry is also useful, but not essential for diagnosis. Methods of fractionating brain homogenates may be used

to rationally classify the tauopathies in a research setting [13]. In the adult brain, there are normally six isoforms of the microtubule-associated protein tau (MAPT): three isoforms with 0, 1, or 2 inserts contain three microtubule-binding repeats (3R tau) and three isoforms, also with 0, 1, or 2 inserts, contain four microtubule-binding repeats (4R tau) [28]. The tauopathies have a biochemical signature: tau protein in these disorders is relatively insoluble and these insoluble species can be detected by biochemical fractionation methods. The insoluble fractions may be further characterized according to the pattern of tau isoforms. For example, in AD, all six isoforms are abnormally hyperphosphorylated and migrate as three major bands and one minor band when visualized by immunoblotting. Treatment with the enzyme alkaline phosphatase removes phosphate groups, and the tau isoforms appear as six bands (3R and 4R tau). This biochemical signature may be used to distinguish AD from the FTLD tauopathies [13]. Thus, brain tissue from patients with FTLD where Pick bodies are present is characterized biochemically by predominantly 3R tau, while CBD, PSP, argyrophilic grain disease (AGD), and sporadic multiple system tauopathy with dementia (MSTD) are predominantly 4R tauopathies [13, 74], and neurofibrillary tangle dementia (NTD), also called tangle predominant form of senile dementia, has inclusions containing a mixture of 3R and 4R tau [34, 35]. FTLD with *MAPT* mutation, of which more than 40 have been described, is biochemically heterogeneous with different mutations being associated with 3R, 4R, or 3R and 4R tauopathy [15]. Monoclonal antibodies, which discriminate between 3R and 4R tau [22] are now commercially available; so, the molecular classification of tauopathies by isoform type may be easily undertaken in the histology laboratory that does not have access to biochemistry.

FTLD with ubiquitin-positive, tau-negative inclusions (FTLD-U), also known as FTLD with MND-type inclusions or MND inclusion dementia, is the most common underlying pathology in FTLD with and without clinical MND [45, 73]. TAR DNA-binding protein 43 (TDP-43), a nuclear protein implicated in exon skipping and transcription regulation, was recently identified as a major protein component of the ubiquitin-immunoreactive inclusions characteristic of sporadic and familial FTLD-U, with and without clinical MND, as well as in sporadic ALS [3, 16, 21, 61]. Biochemistry in these disorders shows TDP-43 to be abnormally phosphorylated, ubiquitinated and cleaved to generate C-terminal fragments, and is recovered only from areas with ubiquitin-immunoreactive inclusions including hippocampus, neocortex, and spinal cord [61]. The neuropathology of these conditions is characterized by ubiquitin- and TDP-43-positive neuronal cytoplasmic inclusions (NCIs), neuronal intranuclear inclusions (NIIs), dystrophic neurites (DNs), and glial cytoplasmic inclusions (GCIs) that are negative for tau, α -synuclein, β -amyloid, neuronal

intermediate filaments, and expanded polyglutamines [21, 61]. The variability in the morphologic types of neuronal inclusions, their distribution, density, and immunohistochemical profile has led to the proposed classification of FTLD-U into four pathologic subtypes [16, 63, 66]. Recently, mutations in the *progranulin* (*PGRN*) gene [4, 20, 57], the molecular genetic basis of non-tau familial FTD linked to chromosome 17, were discovered. The neuropathology in these cases is FTLD-U with ubiquitin-positive neurites, NCIs and, most characteristically, NIIs [4, 50] (but see ref. [37]). However, NIIs can be seen in other FTLD-U cases where *PGRN* mutations are not found [16] and therefore such NIIs cannot be considered pathognomonic for *PGRN* or other (i.e., *valosin-containing protein* *VCP*) mutations associated with FTLD. As demonstrated by IHC and biochemistry, the ubiquitinated pathologic protein in these cases is not progranulin, but TDP-43 [4, 57]. Pathologic TDP-43 is detected biochemically in both affected gray and white matter, suggesting that both glial and neuronal pathology may contribute to the pathogenesis of FTLD-U caused by *PGRN* mutations [61].

Frontotemporal lobar degeneration with *VCP* gene mutation, also called inclusion body myopathy associated with Paget's disease of bone and frontotemporal dementia (IBMPFD), is a rare autosomal dominant disorder caused by mutations in the *VCP* gene [77]. *VCP*, a member of the AAA-ATPase gene super family (ATPase associated with diverse cellular activities), has multiple cellular functions including acting as a molecular chaperone in endoplasmic reticulum-associated protein degradation, stress response, programmed cell death, and interactions with the ubiquitin-proteasome system. The neuropathology in FTLD with *VCP* mutation is a unique subtype of FTLD-U and is characterized by numerous NIIs and relatively few NCIs and DNs [26]; the ubiquitinated inclusions are not primarily composed of the mutated protein (*VCP*), but rather TDP-43 [26, 63].

Frontotemporal lobar degeneration with *charged multivesicular body protein 2B* (*CHMP2B*) gene mutation is the cause of FTD linked to chromosome 3 in a large Danish pedigree [68]. Human *CHMP2B* is a component of the endosomal secretory complex, which becomes dysregulated by the gene defects. Recent studies have revealed ubiquitin-positive, but TDP-43 negative, NCIs in the frontal neocortex and hippocampus, so that this disease is an FTLD-U, but not a TDP-43, proteinopathy [16].

A genetic locus on chromosome 9p for familial FTD-MND has been described [56]. In one family, candidate gene sequencing revealed the presence of a putative disease segregating stop codon mutation (Q342X) in the *intraflagellar transport protein 74* (*IFT74*) gene [55]. *IFT74* is a protein that localizes to the intracellular vesicle compartment and is a component of the intraflagellar transport system responsible for vesicular transport of material synthesized

within the cell body into and along dendrites and axons. Neuropathology in a single case with the *IFT74* mutation was reported as showing all the stigmata of FTLD-U (ubiquitinated NCIs, DNs, and NIIs) and TDP-43 proteinopathy similar to that seen in other reported families with FTD, with or without MND linked to chromosome 9p [16]. Nonetheless, it remains to be established in other families and patients that *IFT74* is indeed a true locus for FTLD.

Neuropathologic classification of FTLDs

Following the principles of the previous consensus criteria for the neuropathologic diagnosis of FTLD [53], and the consensus criteria for the postmortem diagnosis of AD [18] and DLB [52], we acknowledge that only probabilistic statements can be made as to the causal relationship between the neuropathology and the clinical phenotype. Just as the constellation of clinical symptoms associated with FTD, SD, or PNFA do not predict reliably the underlying causative neurodegenerative disease, the presence of the neuropathology of FTLD does not predict with certainty one or other of the clinical phenotypes associated with FTLD, or even if the subject was demented. Small series of cases are inadequate to reliably and robustly determine clinico-pathologic correlations with any one form of FTLD. Multi-center collaborations are beginning to address this challenge [25], and it is only by pooling relatively rare cases from several research centers that reliable clinico-pathologic correlations are likely to emerge.

The neuropathologic criteria proposed here (Table 1) are an evolution of the 2001 criteria proposed by McKhann et al. [53], and take into account more recent descriptions of novel disease entities [6, 14], the discovery of causative gene defects (*PGRN*, *VCP*, *CHMP2B*) and linkage to chromosome 9p [4, 5, 20, 55, 56, 57, 68, 75, 77], and the novel (TDP-43) proteinopathy, which is present in most cases of FTLD-U with or without MND [3, 16, 21, 61]. The neuropathologic diagnosis of FTLD requires the exclusion of other neurodegenerative and systemic diseases, tumors, and drugs of abuse, which may cause a clinical FTLD phenotype. The proposed rational classification of neurodegenerative diseases associated with a clinical FTLD phenotype comprises seven distinct neurohistological types, and is based on the underlying molecular pathology as far as it is known.

Algorithm for the neuropathologic diagnosis of FTLD

The proposed criteria for the neuropathologic diagnosis and nosology of FTLD builds on, and extends, the existing criteria to include neuropathologic assessment using disease-specific antibodies, biochemistry, and molecular genetics to

Table 1 Comparison between the present proposed criteria and McKhann et al. [3] neuropathologic diagnostic criteria for FTLD

Present criteria	McKhann et al. criteria
1. Tauopathy (with associated neuron loss and gliosis) and insoluble tau with a predominance of 3R tau, the most likely diagnoses are: FTLD with Pick bodies FTLD with <i>MAPT</i> mutation	1. When the predominant neuropathological abnormalities are tau-positive inclusions (with associated neuron loss and gliosis) and insoluble tau has a predominance of tau with three microtubule-binding repeats, the most likely diagnoses are: (a) Pick disease (b) Frontotemporal dementia with parkinsonism linked to chromosome 17 (c) Other as yet unidentified familial and sporadic frontotemporal disorders
2. Tauopathy (with associated neuron loss and gliosis) and insoluble tau with a predominance of 4R tau, the most likely diagnoses are: Corticobasal degeneration Progressive supranuclear palsy Argyrophilic grain disease Sporadic multiple system tauopathy with dementia FTLD with <i>MAPT</i> mutation	2. When the predominant neuropathological abnormalities are tau-positive inclusions (with associated neuron loss and gliosis) and insoluble tau has a predominance of four microtubule-binding repeats, the most likely diagnoses are: (a) Corticobasal degeneration (b) Progressive supranuclear palsy (c) Frontotemporal dementia with parkinsonism linked to chromosome 17 (d) Other as yet unidentified familial and sporadic frontotemporal disorders
3. Tauopathy (with associated neuron loss and gliosis) and insoluble tau, with a predominance of 3R and 4R tau, the most likely diagnoses are: Neurofibrillary tangle dementia FTLD with <i>MAPT</i> mutation	3. When the predominant neuropathological abnormalities are tau-positive inclusions (with associated neuron loss and gliosis) and insoluble tau has a predominance of three and four microtubule-binding repeats, the most likely diagnoses are: (a) Neurofibrillary tangle dementia (b) Frontotemporal dementia with parkinsonism linked to chromosome 17 (c) Other as yet unidentified familial and sporadic frontotemporal disorders
4. Frontotemporal neuronal loss and gliosis without tau- or ubiquitin/P62-positive inclusions, the most likely diagnosis is: FTLD (also known as dementia lacking distinctive histologic features)	4. When the predominant neuropathological abnormalities are frontotemporal neuronal loss and gliosis without tau- or ubiquitin-positive inclusions and without detectable amounts of insoluble tau, the most likely diagnoses are: (a) Frontotemporal lobar degeneration (also known as dementia lacking distinct histopathological features) (b) Other as yet unidentified familial and sporadic frontotemporal disorders
5. TDP-43 proteinopathy with associated neuronal loss and ubiquitin-positive/P62-positive, tau-negative inclusions, with MND or without MND but with MND-type inclusions, the most likely diagnoses are: FTLD-U with MND (FTLD-U types 1–3) FTLD-U but without MND (FTLD-U types 1–3) FTLD-U with <i>PGRN</i> mutation (FTLD-U type 3) FTLD-U with <i>VCP</i> mutation (FTLD-U type 4) FTLD-U linked to chromosome 9p (FTLD-U type 2) Other as yet unidentified TDP-43 proteinopathies	5. When the predominant neuropathological abnormalities are frontotemporal neuronal loss and gliosis with ubiquitin-positive, tau-negative inclusions and without detectable amounts of insoluble tau, with MND or without MND but with MND-type inclusions, the most likely diagnoses are: (a) Frontotemporal lobar degeneration with MND (b) Frontotemporal lobar degeneration with MND-type inclusions but without MND, or (c) Other as yet unidentified familial and sporadic frontotemporal disorders.

Table 1 continued

Present criteria McKhann et al. criteria

6. Frontotemporal neuronal loss and gliosis with ubiquitin-positive/P62-positive, TDP-43- and tau-negative inclusions, the most likely diagnoses are:

FTLD-U with *CHMP2B* mutation

Basophilic inclusion body disease (BIBD)

Other as yet unidentified FTLD-U, non-TDP-43 proteinopathies

7. Frontotemporal neuronal loss and gliosis with ubiquitin/P62 and α -internexin-positive inclusions, the most likely diagnosis is:

Neuronal intermediate filament inclusion disease (NIFID)

CHMP2B charged multivesicular body protein 2B gene, *FTLD* frontotemporal lobar degeneration, *FTLD-U* FTLD with ubiquitin-positive, tau-, α -synuclein-, TDP-43-, and neuronal intermediate filament protein-negative inclusions, *MAPT* microtubule-associated protein tau gene, *MND* motor neuron disease, neurofibrillary tangle dementia, also called tangle predominant form of senile dementia, *PGRN* progranulin gene, *TDP-43* TAR DNA-binding protein 43, *VCP* valosin-containing protein gene

FTLD Protocol Flowchart

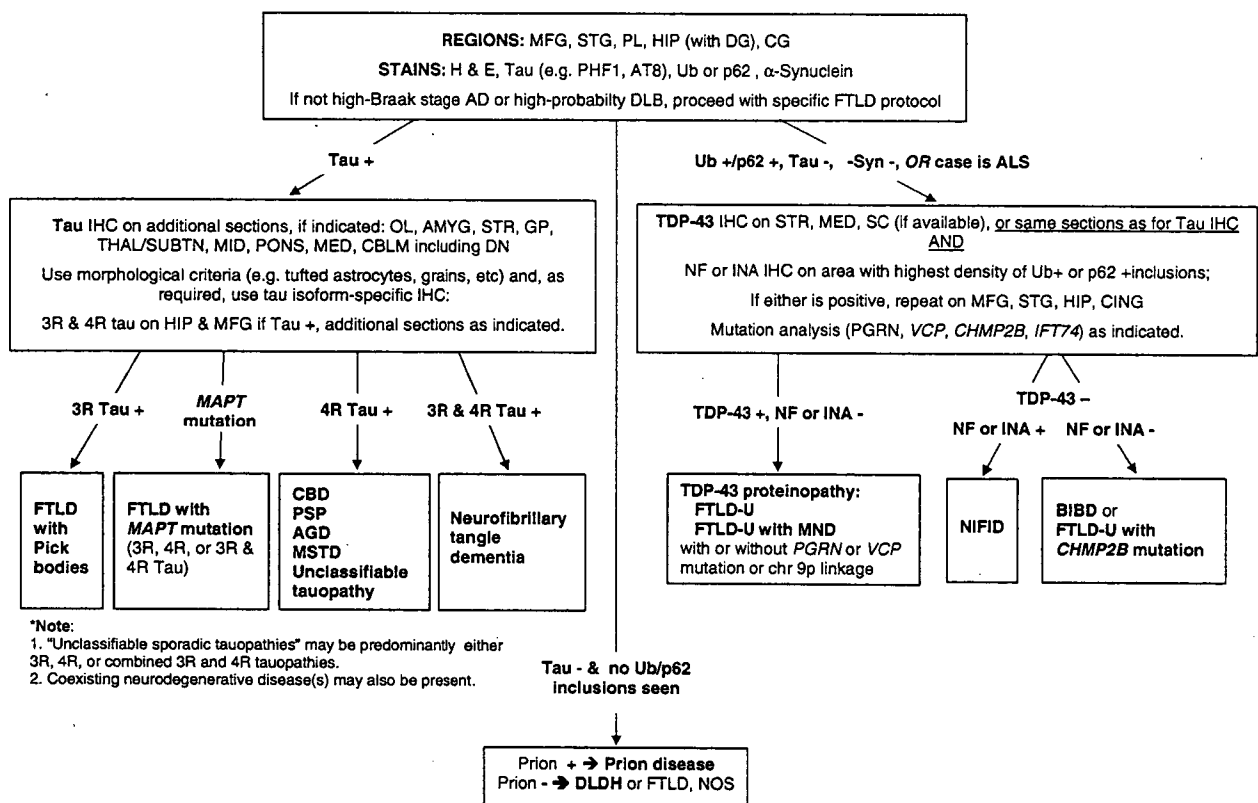


Fig. 1 Frontotemporal lobar degeneration neuropathology algorithm flow chart. *AD* Alzheimer’s disease, *AGD* argyrophilic grain disease, *AMYG* amygdala, *BIBD* basophilic inclusion body disease, *CBD* corticobasal degeneration, *CBLM* cerebellum including the dentate nucleus (*DN*), *CHMP2B* charged multivesicular body protein 2B gene, *CG* cingulate gyrus, *DLB* dementia with Lewy bodies, *DLDH* dementia lacking distinctive histologic features, also called FTLD according to McKhann et al. [4] criteria, *FTLD* frontotemporal lobar degeneration, *FTLD-U* FTLD with ubiquitin-positive, tau-negative inclusions, *GP* globus pallidus, *H&E* hematoxylin and eosin, *HIP* hippocampus, *IHC* immunohistochemistry, *INA* α -internexin, *MAPT* microtubule-associated protein tau gene, *MED* medulla oblongata, *MFG* middle

frontal gyrus, *MID* midbrain including the substantia nigra, *MND* motor neuron disease, *MSTD* sporadic multiple system tauopathy with dementia, *NIFID* neuronal intermediate filament inclusion disease, *NF* neurofilament; neurofibrillary tangle dementia, also called tangle predominant form of senile dementia, *NOS* not otherwise specified, *OL* occipital lobe, *PGRN* progranulin gene, *FL* frontal lobe, *PL* parietal lobe, *PSP* progressive supranuclear palsy, *SC* spinal cord, *STG* superior temporal gyrus, *STR* striatum, *TDP-43* TAR DNA-binding protein 43, *THAL/SUBTN* thalamus and subthalamic nucleus, *Ub* ubiquitin, *VCP* valosin-containing protein gene, *3R*, *4R*, or *3R and 4R* tau isoforms containing 3, 4, or 3 and 4 microtubule-binding repeats

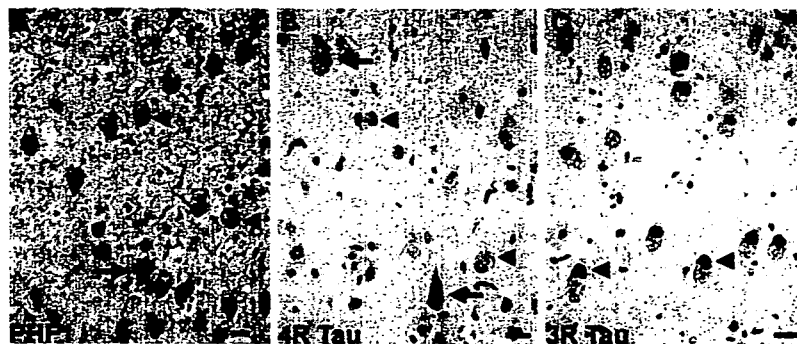
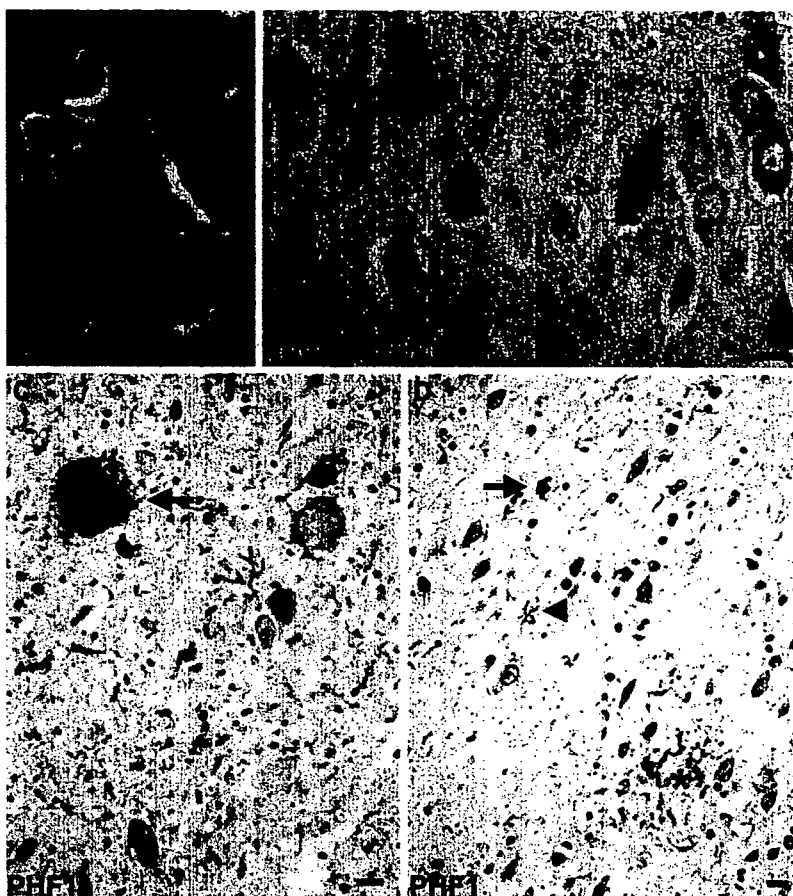


Fig. 2 Frontotemporal lobar degeneration with Pick bodies. Pick bodies (*arrowheads*) and a neurofibrillary tangle (*arrow*) in the subiculum (**a**) are immunolabeled by anti-phosphorylated tau antibodies (*PHF1* immunohistochemistry). Pick bodies are not immunolabeled

with anti-4R tau antibodies (*arrowheads*), while neurofibrillary tangles are immunolabeled (*arrows*) (**b**). Anti-3R tau antibodies clearly label Pick bodies (*arrowheads*) (**c**). **b** 4R tau (ET3) and **c** 3R tau (RD3) immunohistochemistry. Bars 10 μ m

Fig. 3 Corticobasal degeneration. **a** A swollen achromatic neuron (*arrow*) in the middle frontal gyrus. Hematoxylin and eosin (*HE*). **b** Tau-positive neurofibrillary tangles in the pyramidal neurons of the CA1 hippocampal subfield. **c** A globose neurofibrillary tangle (*arrow*) in the locus coeruleus. **d** An astrocytic plaque (*asterisk*), coiled body (*arrow*), and threads (*arrowhead*) in the deep cortical laminae and white matter of the parietal lobe. **b**, **c**, **d** Anti-phosphorylated tau (*PHF1*) immunohistochemistry. Bars 10 μ m

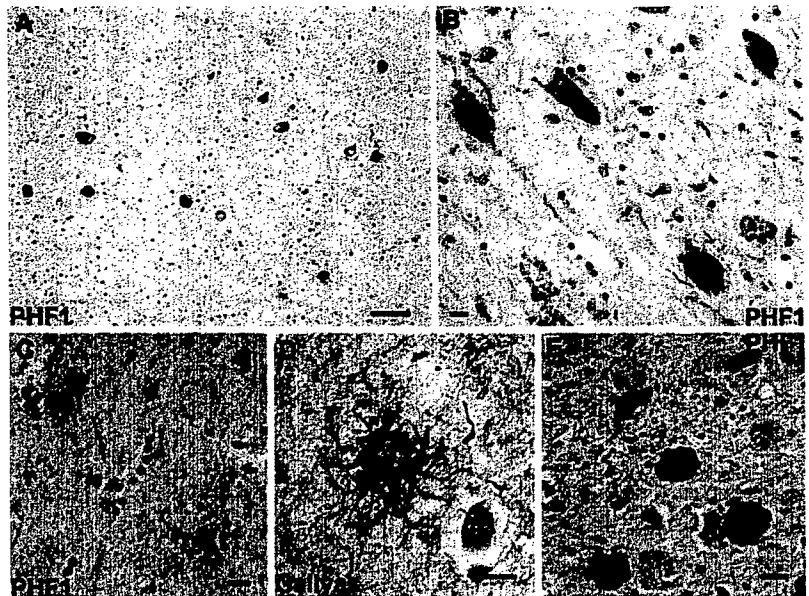


arrive at the neuropathologic diagnosis of one of the disease entities causing FTL. It is appreciated that it may not be practical, possible, or even necessary, to undertake sophisticated neuroanatomical investigations of neuron and synapse density, biochemistry or molecular genetics in every case. For these reasons, the following neuropathologic algorithm has been developed, which should be feasible at most dementia research centers. It is envisaged that this

algorithm, with its inbuilt criteria for diagnosis, will supersede existing neuropathologic criteria [3], and become the standard operational protocol for the working neuropathologic diagnosis of FTL (Figs. 1, 2, 3, 4, 5, 6, 7, 8, 9, 10, 11, 12, 13, 14).

Recently, staging schemes have been developed that no longer rely on capricious silver impregnation methods, but employ instead sensitive monoclonal and polyclonal

Fig. 4 Progressive supranuclear palsy. Neurofibrillary tangles in the subthalamic nucleus (a), oculomotor nucleus (b), and locus coeruleus (e). Tufted astrocytes in the putamen (c and d). a, b, c, e Anti-phosphorylated tau (PHF1) immunohistochemistry. d *Galylas* silver impregnation. Scale bars a 50 μ m, b, c, d, e 10 μ m



antibodies that detect, by IHC, the pathologic proteins of the major neurodegenerative diseases [9, 10, 52]. Multi-center studies have confirmed the reproducibility and reliability of IHC over traditional staining methods, and IHC is recommended for the detection of the signature lesions of FTLD [1, 53], when appropriate. Thus, neurodegenerative diseases with α -synuclein pathology, with or without A β plaques and tau-positive neurofibrillary tangle (AD) pathology (i.e., DLB, Parkinson's disease, and multiple system atrophy), or those with plaque and tangle pathology (i.e. Alzheimer disease) are excluded using established sampling schemes and diagnostic criteria for these diseases [18, 52].

Tau-positive inclusions

Where neurofibrillary tangles alone are present, in the absence of A β plaques, in the context of neuronal loss and gliosis, NTD, also called tangle predominant form of senile dementia, which, like AD tangles, contain tau composed of all six isoforms, is a diagnostic possibility. Where the distribution of neuronal and glial tau pathology is more widespread and includes frontal, temporal, and parietal neocortex, basal ganglia, and brainstem nuclei, then sporadic MSTD may be indicated [6]. Neurofibrillary tangles in more subcortical regions including the basal ganglia, subthalamic nucleus, midbrain, and pontine nuclei indicate progressive supranuclear palsy [31, 72]. Distinguishing lesions in PSP are tau-positive tufted astrocytes and are found in affected neocortical and subcortical regions. Corticobasal degeneration is characterized by frontal and temporal atrophy that is not infrequently asymmetric, neuronal

loss, gliosis, swollen achromatic neurons that are faintly tau-positive, and tau-positive neurofibrillary tangles in the neocortex, basal ganglia, and brainstem nuclei [24, 27]. Distinguishing lesions in CBD are tau-positive astrocytic plaques and threads found in the affected neocortex and subcortical white matter and in the basal ganglia. In both PSP and CBD, tau-positive oligodendroglial inclusions called coiled bodies are seen, but these are generally at a lower density than inclusions in astrocytes. Tau-positive ovoid structures (glial processes), astrocytes, and oligodendroglial inclusions (coiled bodies), when confined to the medial temporal lobe and limbic structures, indicate another tauopathy, AGD [7]. If globose tau-positive NCIs, called Pick bodies, are present in the non-pyramidal (dentate gyrus granule cells) and pyramidal neurons of area CA1 of the hippocampus, and pyramidal neurons of the temporal and frontal lobes, then FTLD with Pick bodies may be present [80]. Pick bodies are largely or wholly composed of 3R tau, which can be demonstrated by IHC or immunoblotting, while the tau-positive inclusions of PSP, CBD, MSTD, and AGD all contain 4R tau indicating that these latter disorders may represent a spectrum of 4R tauopathies [13, 74]. Finally, FTLD with *MAPT* mutation, also called FTD with parkinsonism linked to chromosome 17 (FTDP-17), is not only clinically and genetically heterogeneous (more than 40 mutations have been reported in the *MAPT* gene), but is also neuropathologically heterogeneous. The spectrum of neuronal and glial pathology seen in 3R, 4R, and combined 3R and 4R tauopathies is also found in such cases of familial tauopathy [15, 44, 70]. For the practicing neuropathologist, the presence of this spectrum of pathology in a case warrants further genetic investigation particularly if there is an autosomal dominant pattern of

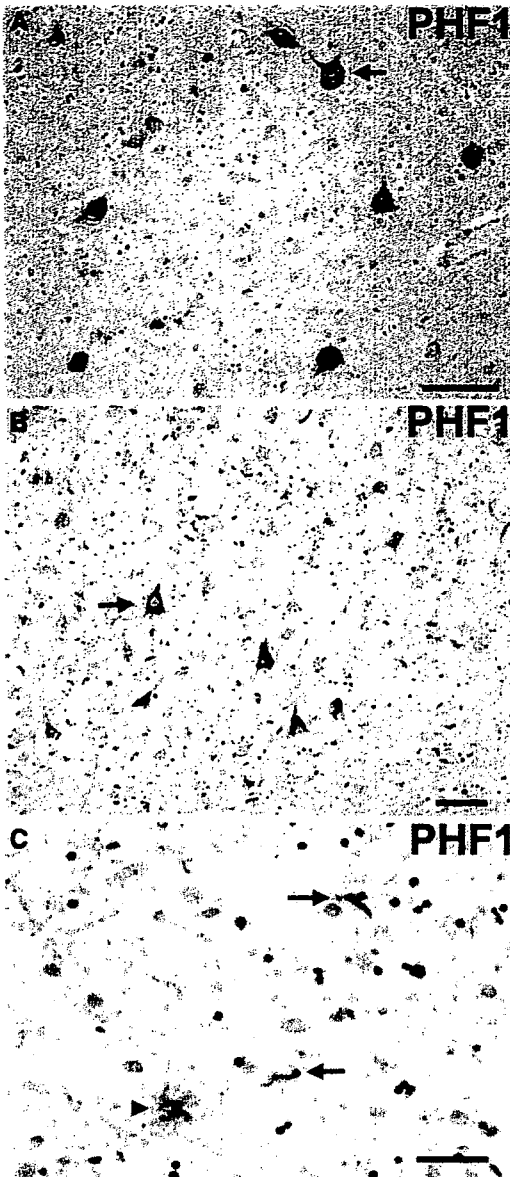


Fig. 5 Argyrophilic grain disease. **A** Swollen achromatic neuron (*arrow*) with pale center and more intense tau-immunoreactive periphery in the subiculum. Tau-immunoreactive grains in the neuropil and diffusely stained pyramidal neurons (*arrow*) indicating a pre-neurofibrillary tangle stage in the pyramidal layer of the hippocampus (**B**). **A** tau-immunoreactive astrocytic inclusion (*arrowhead*) and oligodendroglial cytoplasmic inclusions called coiled bodies (*arrows*) in the CA1 subfield of the hippocampus. (**a, b, c**) Anti-phosphorylated tau (*PHF1*) immunohistochemistry. *Scale bars* (**a**) 100 μ m and (**b** and **c**) 50 μ m

inheritance. Similar 3R and 4R tau heterogeneity is seen in some tauopathies that cannot be categorized as FTLTD with Pick bodies, PSP, CBD, or AGD, and in individuals without *MAPT* mutations. Such a case may have tau pathology in the distribution described in sporadic MSTD, or may have to be categorized as “unclassifiable sporadic tauopathy.”

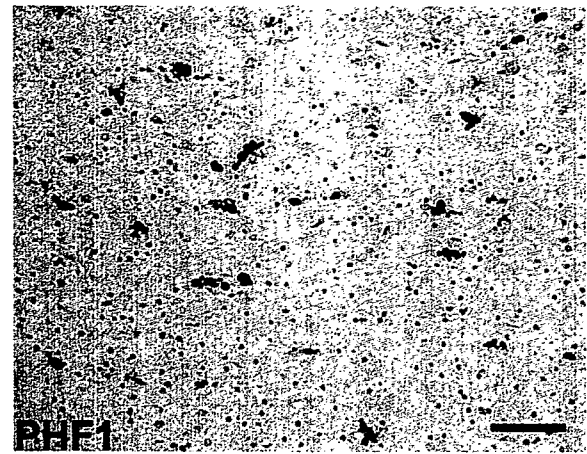


Fig. 6 Sporadic multiple system tauopathy with dementia. Neuronal and glial globular inclusions at the gray/white junction. Anti-phosphorylated tau (*PHF1*) immunohistochemistry. *Scale bar* 100 μ m

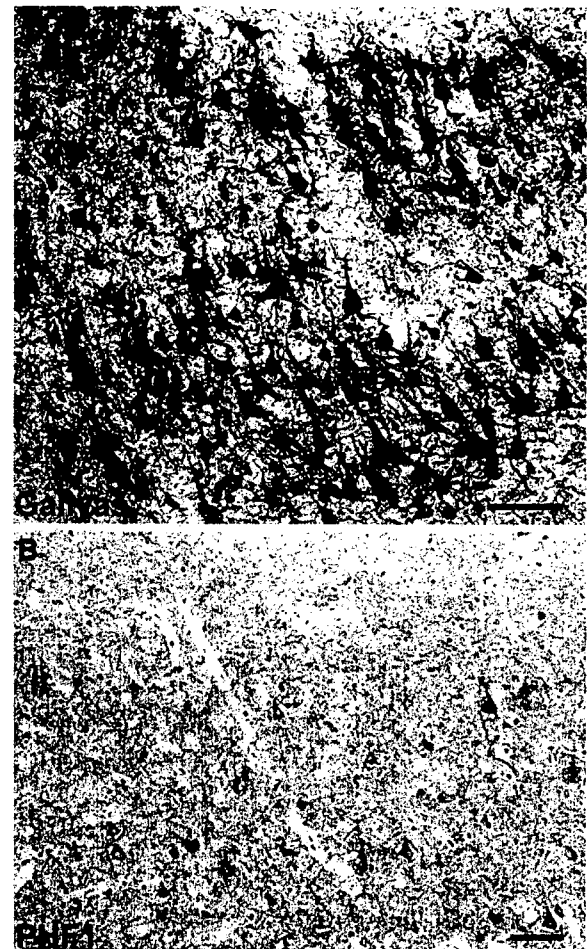


Fig. 7 Neurofibrillary tangle dementia. **a, b** Numerous neurofibrillary tangles in the upper and lower pyramidal neurons of the occipitotemporal cortex; no neuritic plaques or amyloid deposits are present. **a** *Gallyas* silver impregnation. **b** Anti-phosphorylated tau (*PHF1*) immunohistochemistry. *Scale bars* 50 μ m

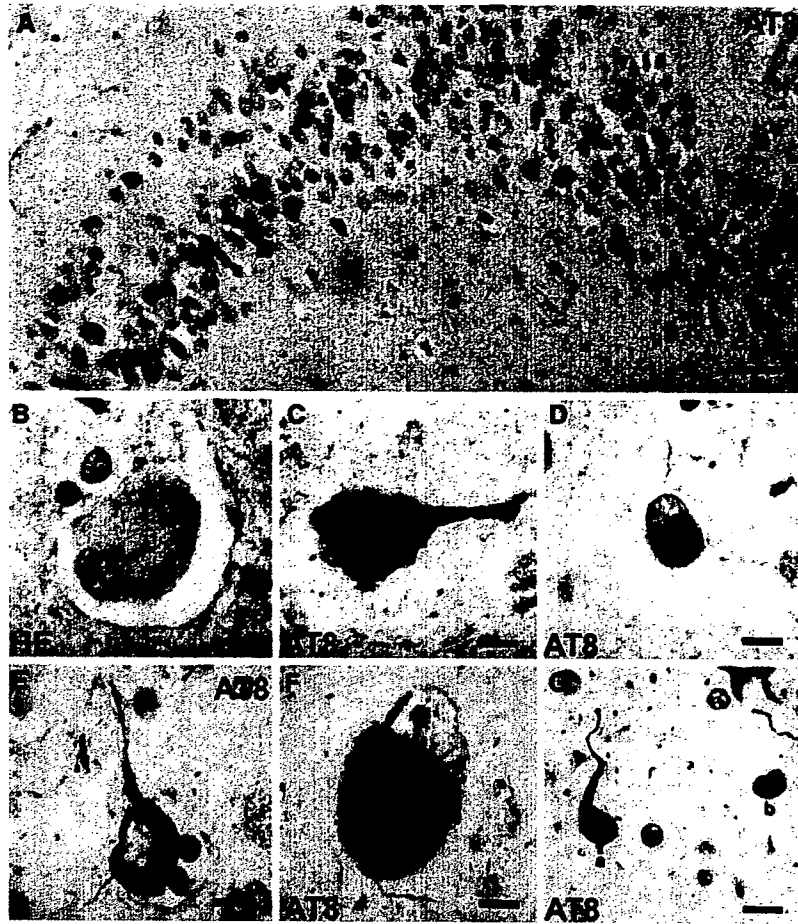


Fig. 8 Frontotemporal lobar degeneration (FTLD) with *MAPT* mutation. Inclusions in FTLD with *MAPT* G389R mutation (a) and FTLD with *MAPT* intron 10 + 16 mutation (b–g). a Numerous tau-immunoreactive Pick body-like inclusions in the granule neurons of the dentate fascia. b A swollen achromatic neuron in the superior temporal gyrus. c A swollen neuron with a central area of pale anti-tau immunoreactivity surrounded by more intense staining. Fibrillary material surrounds the nucleus and extends into the apical dendrite. d An intraneuronal

inclusion resembling a Pick body in the superior frontal gyrus. e A neurofibrillary tangle-like inclusion in layer V of the superior frontal gyrus. f A globose neurofibrillary tangle-like inclusion in the dorsal raphe nucleus. g An astrocytic fibrillary inclusion (a) and a coiled body (b) in an oligodendrocyte in the white matter of the frontal lobe. b Hematoxylin and eosin (HE); (a, c–g) anti-phosphorylated tau (AT8) immunohistochemistry. Scale bars 10 μ m. (Adapted from Ref. [44]; reproduced with permission)

Tau-negative, ubiquitin-positive inclusions

TDP-43 proteinopathy

Immunohistochemistry for ubiquitin, P62, and TDP-43 in cases with FTLD generally reveals similar pathology that includes a spectrum of neuronal (NCIs, DNs, and NIIs) and glial, predominantly oligodendroglial, cytoplasmic inclusions (GCIs) [62, 61]. However, there are significant differences in the immunohistochemical findings with ubiquitin, P62, and TDP-43. Ubiquitin immunoreactivity is present in extensive age-related pathology in gray and white matter, e.g., dot-like bodies and granular degeneration of myelin, which can mask subtle neuronal and glial pathology and can be difficult to interpret. P62 immunostaining detects the same range of pathological structures as anti-ubiquitin, but

highlights less age-related pathology, making interpretation somewhat less demanding. TDP-43 immunoreactivity is present in nuclei of most cells types and changes in distribution within affected neurons in disease. Screening cases using TDP-43 immunostaining as a primary diagnostic tool, as might be used for tau and α -synuclein accumulations, is more demanding. Four histologic subtypes of FTLD-U have been proposed, based on the predominant type of inclusion present as detected using anti-ubiquitin, its distribution in the cortex, and density [16, 63, 66]. Other types have been proposed as well and take into account involvement of other brain regions (e.g., hippocampus or corpus striatum) and the morphology of the lesions [2, 38]. Patterns of FTLD-U histology based solely on cortical pathology include a system proposed by Sampathu et al. [66], and Neumann et al. [63]; while Mackenzie et al. [49]

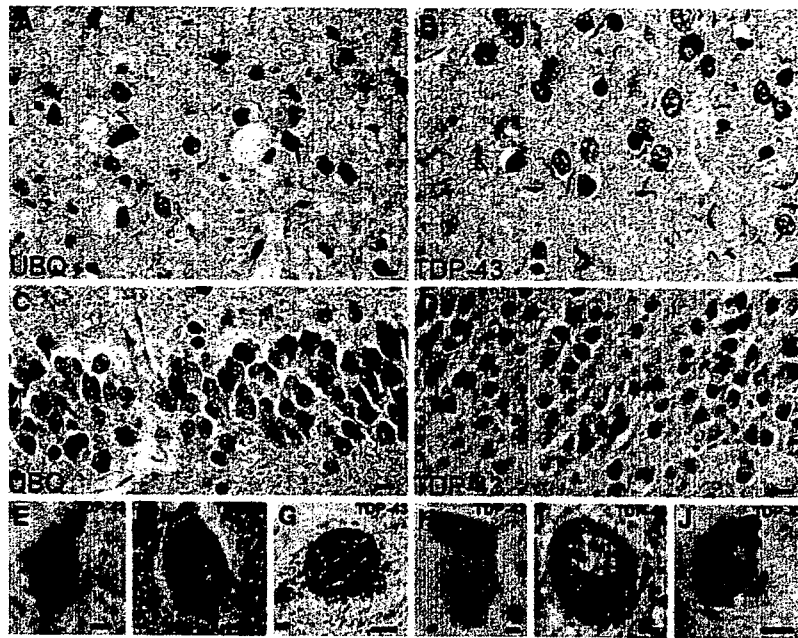


Fig. 9 Frontotemporal lobar degeneration (FTLD)-U with or without MND: spectrum of *TDP-43* pathology. Adjacent sections of superficial frontal neocortex showing neuronal cytoplasmic inclusions (NCIs), dystrophic neurites (DNs), and isolated neuronal intranuclear inclusions (NIIs) stain for both ubiquitin (a) and *TDP-43* (b). NCI in the dentate granule cells stain for ubiquitin (c) and *TDP-43* (d). Neuronal

and glial inclusions include NCI (e), round and lentiform NIIs (f, g); skein-like (h), and compact round (i) NCI in the lower motor neurons; and glial cytoplasmic inclusion (GCI) (j). (a and c) ubiquitin immunohistochemistry (b, d, e–j) *TDP-43* immunohistochemistry). Scale bars 10 μ m (a–d); 5 μ m (e–j) (Adapted from Ref. [16]; reproduced with permission)

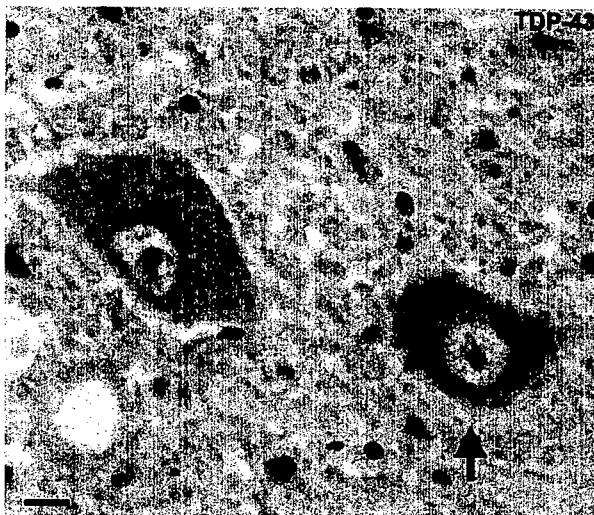


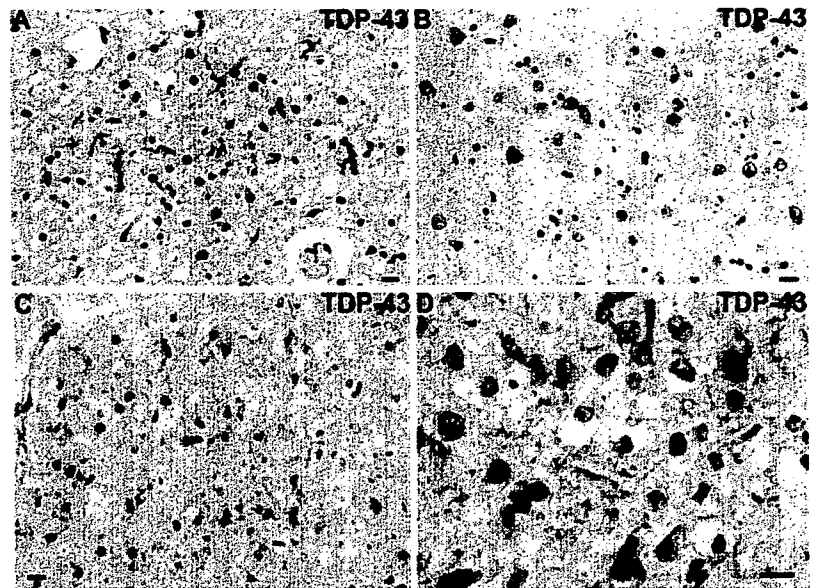
Fig. 10 Frontotemporal lobar degeneration-U with MND. Diffuse perinuclear staining in a motor neuron (arrow). *TDP-43* immunohistochemistry. Scale bar 10 μ m

have proposed a system that includes cortical and dentate fascia inclusions. In all these schemes the same descriptors were employed to differentiate subtypes, though the numbering of each subtype differed among schemes. In the present composite scheme, type 1 cases (as in [66], but known as type 2 in Mackenzie et al. [49]) are characterized

by an abundance of long DN, predominantly in the superficial cortical laminae, with few or no NCIs or NIIs. Type 2 cases (as in [66], but known as type 3 in Mackenzie et al. [49]) are characterized by numerous NCIs in both superficial and deep cortical laminae as well as infrequent DN and sparse or no NIIs. Type 3 cases (as in [66], but known as type 1 in Mackenzie et al. [49]) are characterized by pathology predominantly in the superficial cortical layers with numerous NCIs, DN, and variable numbers of NIIs. Type 4 cases [16, 63] are distinguished by numerous NIIs and infrequent NCIs and DN in the neocortical areas with relative sparing of the hippocampus, consistent with the pathology described in cases of FTLD with *VCP* mutations (but see ref. [30]). Consensus on the validity, reliability, and reproducibility of the various proposed typing schemes, as well as their clinical significance, remain to be determined.

If *TDP-43*- and ubiquitin- or P62-positive, tau- and α -synuclein-negative inclusions are found in the superficial laminae of the frontal and temporal neocortex and neurons of the dentate gyrus, the most likely diagnosis is FTLD-U [21, 36, 45]. If in addition, there is *TDP-43* proteinopathy and ubiquitin-positive inclusions in the lower motor neurons and evidence of motor neuron loss, gliosis, Bunina bodies, and corticospinal tract degeneration, FTLD with MND is the most likely diagnosis [53, 64, 79].

Fig. 11 Frontotemporal lobar degeneration-U, subtypes 1–4. **a–d** Type 1 is characterized by long and tortuous dystrophic neurites (DNs) in laminae II/III with relatively few neuronal cytoplasmic inclusions (NCIs) and no neuronal intranuclear inclusion (NII). **b** Type 2 has numerous NCIs, relatively few DNs, and no NII is present. **c** Type 3 has numerous NCIs and DNs and an occasional NII in lamina II. **d** Type 4 pathology in a case of FTD with *VCP* mutation is characterized by numerous NII and DN, but few NCI. *TDP-43* immunohistochemistry. Scale bar 10 μ m (**a–d**). (Adapted from Ref. [14]; reproduced with permission)



There is heuristic value in the sub-classification of FTLD-U beyond pathologic description alone, with clinical and genetic correlates of histologic patterns emerging. Cases with type 1 histology are associated with SD, whereas cases of FTLD with MND frequently show type 2 histology [49]. In genetic terms, cases with *PGRN* or *VCP* gene mutations, and in cases linked to chromosome 9, distinct patterns of ubiquitin- and TDP-43-positive inclusions are also seen. FTLD with *PGRN* mutation cases often display a PNFA clinical phenotype and exclusively show type 3 histology [16], whereas those with *VCP* mutations have type 4 histology. Cases linked to chromosome 9 have type 2 histology [16] and the majority of such cases also have ubiquitin- and TDP-positive inclusions in the upper and lower motor neurons, identical to those encountered in sporadic MND [16] or sporadic FTLD with MND where a similar type 2 histology is often present [49]. These latter data indicate that the pathology of FTLD linked to chromosome 9p is a specific subtype of FTLD-U (type 2) and that TDP-43 is the disease-associated protein. Biochemistry of sporadic cases of FTLD with and without MND, cases of sporadic ALS, and familial cases of FTLD-U with *PGRN* and *VCP* mutations, and those linked to chromosome 9p, all have a characteristic biochemical signature: TDP-43 is detected in the detergent-insoluble urea fractions from affected regions and is abnormally phosphorylated, with additional protein bands of ~25 and 45 kDa, as well as a high molecular smear, and is ubiquitinated [16, 61, 62, 63]. The quantity of these modified TDP-43 species detected by biochemistry [62, 63] may be variable, but correlates with the amount of pathology detected by IHC. Additionally, the 45 kDa species collapse into a 43 kDa band upon dephosphorylation with alkaline phosphatase, indicating that TDP-43 is abnormally phosphorylated, with features paralleling

the biochemical changes seen in the tauopathies. Hippocampal sclerosis (HS) may be found as a coexisting pathology in FTLD-U with or without MND, and small numbers of ubiquitin- and TDP-43-positive inclusions may be seen exclusively in the dentate granule cells. Preliminary data indicate that some, or perhaps most, cases of HS are TDP-43 proteinopathies [2], but further studies on larger samples of “pure HS” and biochemical studies are required to determine the nosologic status of HS.

TDP-43-negative inclusions

In those cases that have ubiquitin- or P62-positive, TDP-43-, tau-, and α -internexin-negative NCIs in the frontal and temporal lobes and dentate gyrus, the most likely diagnosis is FTLD with *CHMP2B* mutation [16]. Mutations in the *CHMP2B* gene are the cause of FTD-linked to chromosome 3 in a large Danish pedigree [68]. Human *CHMP2B* is a component of the endosomal secretory complex, which becomes dysregulated by the gene defect. However, the absence of DN and the presence of granular, ubiquitin-positive structures within the neocortex of these cases distinguish this FTLD-U subtype from the types 1–4 described above. Thus, based on the small number of cases studied to date, familial FTLD with *CHMP2B* mutation appears to be a distinctive pathologic subtype of FTLD-U and is not a TDP-43 proteinopathy on the basis of IHC.

In cases of FTLD where there is frontotemporal neuron loss and gliosis, α -internexin- or neurofilament-positive, TDP-43-, α -synuclein-, and tau-negative, and variably ubiquitinated but P62-positive neuronal inclusions, the most likely diagnosis is neuronal intermediate filament inclusion disease [14]. Where there is FTLD and P62-positive,